

LA-7089-MS

Informal Report

c.4

NRC-4

Liner-Concrete Heat Transfer Study for Nuclear Power Plant Containments



Issued: January 1978



los alamos
scientific laboratory
of the University of California
LOS ALAMOS, NEW MEXICO 87545

An Affirmative Action/Equal Opportunity Employer

UNITED STATES
DEPARTMENT OF ENERGY
CONTRACT W-7403-ENG. 36

This work was supported by the US Nuclear Regulatory Commission's
Office of Nuclear Regulatory Research, Division of Systems Safety.

Printed in the United States of America. Available from
National Technical Information Service
U.S. Department of Commerce
5285 Port Royal Road
Springfield, VA 22161

Mikrofiche	\$ 3.00	126-150	7.25	251-275	10.75	376-400	13.00	501-525	15.25
001-025	4.00	151-175	8.00	276-300	11.00	401-425	13.25	526-550	15.50
026-050	4.50	176-200	9.00	301-325	11.75	426-450	14.00	551-575	16.25
051-075	5.25	201-225	9.25	326-350	12.00	451-475	14.50	576-600	16.50
076-100	6.00	226-250	9.50	351-375	12.50	476-500	15.00	601-up	--1
101-125	6.50								

1. Add \$2.50 for each additional 100-page increment from 601 pages up.

NOTICE

This report was prepared as an account of work sponsored by the United States Government. Neither the United States nor the United States Nuclear Regulatory Commission, nor any of their employees, nor any of their contractors, subcontractors, or their employees, makes any warranty, express or implied, or assumes any legal liability or responsibility for the accuracy, completeness or usefulness of any information, apparatus, product or process disclosed, or represents that its use would not infringe privately owned rights.

LA-7089-MS
Informal Report
NRC-4



Liner-Concrete Heat Transfer Study for Nuclear Power Plant Containments

R. G. Gido

Manuscript completed: December 1977
Issued: January 1978



Prepared for the US Nuclear Regulatory Commission
Office of Nuclear Regulatory Research

CONTENTS

ABSTRACT	-----	1
I. SUMMARY	-----	1
II. INTRODUCTION	-----	2
III. HEAT TRANSFER ANALYSIS	-----	2
A. Analytical Models	-----	3
B. Method of Analysis	-----	3
C. Results	-----	4
1. One-Dimensional Model	-----	4
2. Effects of Radiation, Natural Convec- tion, and Anchors	-----	5
3. Liner-Concrete Conductance vs Gap	-----	7
4. Effect of Displacement Variation	-----	7
5. Combined Effects on Energy Absorbed and on One-Dimensional Liner-Concrete Conductance	-----	8
IV. LINER DISPLACEMENT CONSIDERATIONS	-----	8
V. EFFECT ON CONTAINMENT PRESSURE	-----	9
VI. CONCLUSIONS	-----	11
ACKNOWLEDGMENTS	-----	12
APPENDIX A - MODEL DEFINITION	-----	13
I. MESH SPACING	-----	13
II. CONCRETE DEPTH	-----	14
III. INITIAL TEMPERATURE	-----	15
IV. ATMOSPHERE BOUNDARY CONDITIONS	-----	15
V. CONCRETE PROPERTIES	-----	16
VI. TIME INCREMENT	-----	16
APPENDIX B - EFFECT OF RADIATION ON LINER-CONCRETE HEAT TRANSFER CONDUCTANCE	-----	17
APPENDIX C - EFFECT OF NATURAL CONVECTION ON THE LINER- CONCRETE HEAT TRANSFER CONDUCTANCE	-----	18
REFERENCES	-----	20

FIGURES

1.	Typical dry containment configuration (Ref. 3).	22
2.	Prestressed concrete containment vessel liner (Ref. 4)	23
3.	Two-dimensional analytical model of a represent- ative containment liner, anchor, and concrete region.	24
4.	Containment atmosphere boundary conditions.	25
5.	Examples of extreme variations of liner-concrete displacements (Ref. 5).	26
6.	Effect of H_C on energy/area absorbed for a one- dimensional model.	27
7.	Effect of H_C on temperature distribution at 30 s for the one-dimensional model.	28
8.	Effect of H_C on temperature distribution at 300 s for the one-dimensional model.	29
9.	Effect of time on temperature distribution for $H_C = 57 \text{ W/m}^2/\text{K}$ ($10 \text{ Btu/h/ft}^2/^\circ\text{F}$) for the one- dimensional model.	30
10.	Effect of h_{LC} and h_{AC} on absorbed energy/area for the two-dimensional model.	31
11.	Two-dimensional model temperature distribution with high anchor-concrete conductance.	33
12.	Two-dimensional model temperature distribution with low anchor-concrete conductance.	34
13.	Gap conductance due to conduction and radiation across an air gap.	35
14.	Heat transfer effects on lined-concrete energy absorbed/area, E/A , after 300 s.	36
15.	Heat transfer effects on one-dimensional liner- concrete interfacial conductance, H_C .	37
A-1.	Effect of initial temperature on energy absorbed.	38
A-2.	Two-dimensional energy absorbed with different boundary conditions.	39

FIGURES (cont)

A-3. Two-dimensional model heat fluxes (\dot{E}/A) with
different boundary conditions. - - - - - 40

TABLES

I. Thermal Properties - - - - - 41

II. Determination of the Equivalent One-Dimensional
Liner-Concrete Interface Conductance (H_C) to
Give the Same Absorbed Energy/Area (E/A) as the
Two-Dimensional (with Anchor) Model with Various
Liner-Concrete Interface Conductances (h_{LC}) at
300 s - - - - - 41

III. Effect of Anchors on the Energy Absorbed/Area
vs Time for $h_{LC} = 56.8 \text{ W/m}^2/\text{K}$ ($10 \text{ Btu/h/ft}^2/^\circ\text{F}$) - 42

IV. Air Thermal Conductivity vs Temperature - - - - - 42

V. Effect of Liner Displacement Variation on
Energy Absorbed at 300 s - - - - - 42

A-I. Two-Dimensional Model: Effect of Mesh Spacing
in Direction Normal to Liner - - - - - 43

A-II. One-Dimensional Model: Effect of Mesh Spacing
in Direction Normal to Liner - - - - - 44

A-III. Effect of Transient Time Increment on Energy
Absorbed - - - - - 45

C-I. Vertical Enclosure
Natural Convection Heat Transfer Coefficient - - - 46

LINER-CONCRETE HEAT TRANSFER STUDY
FOR NUCLEAR POWER PLANT CONTAINMENTS

by

R. G. Gido

ABSTRACT

Containment liner-concrete interface heat transfer phenomena have been investigated. In particular, the effects of thermal radiation and natural convection heat transfer as well as the effects of anchors on the liner-concrete conductance were studied. The need for a thorough structural analysis to determine the spatial distribution of the gap between the liner and concrete has been found to be necessary before the liner-concrete conductance can be accurately defined. A reasonable minimum value for a one-dimensional liner-concrete interface conductance of $57 \text{ W/m}^2/\text{K}$ ($10 \text{ Btu/h/ft}^2/^\circ\text{F}$) has been established; reasonable maximum value is $2\,800 \text{ W/m}^2/\text{K}$ ($500 \text{ Btu/h}\cdot\text{ft}^2\cdot^\circ\text{F}$).

I. SUMMARY

Liner-concrete heat transfer for nuclear power plant dry containments was studied to determine the effects of conduction, thermal radiation, and natural convection heat transfer as well as the effects of anchors. These effects can be combined into a one-dimensional liner-concrete heat transfer conductance (H_c) suitable for use in conventional containment transient pressure-temperature response analysis. A key parameter affecting the liner-concrete heat transfer is the gap between the liner and the concrete. The magnitude of this parameter was found to be very difficult to establish. Complicating factors include the geometry and large-scale dimensions, in addition to manufacturing, construction, structural, aging, thermal cycle, and accident transient considerations. As a result, this gap was carried through the analysis as a variable to determine bounding values for H_c . Suitable minimum and maximum values for H_c were found to be $\sim 57 \text{ W/m}^2/\text{K}$ ($10 \text{ Btu/h/ft}^2/^\circ\text{F}$) and $\sim 2\,800 \text{ W/m}^2/\text{K}$ ($500 \text{ Btu/h/ft}^2/^\circ\text{F}$), respectively. Methods of analysis, model definition, and the effects of initial temperature and atmosphere boundary conditions are also described.

II. INTRODUCTION

The purpose of this study is to determine the effects of liner displacement, radiation, natural convection, and anchors on the containment liner-concrete interface heat transfer. The results of this study can be used to evaluate the liner-concrete interface heat transfer conductances, H_C , used in containment transient pressure response analyses as required by the U.S. Nuclear Regulatory Commission (NRC).¹ The interfacial heat transfer conductance, as used in this text, is defined by,

$$H_C = \frac{Q}{A\Delta T}$$

where

Q = energy flow rate,

A = area, and

ΔT = temperature difference,

and is equivalent to what is also called interfacial heat transfer coefficient, thermal contact coefficient, and the inverse of the thermal resistance.

A suitable representation of the liner-concrete heat transfer is important because it affects the energy absorbed by the lined-concrete containment structures and therefore the pressures and temperatures obtained from containment pressure-temperature response analyses. These analyses usually utilize a simple one-dimensional representation for the lined-concrete containment structures.² Another objective of this study is to provide guidelines for bounding values of the liner-concrete interface heat transfer conductances to be used in these one-dimensional representations.

The location and description of the liner-concrete interface under consideration is provided by Figs. 1 and 2.^{3,4} Such dry containments are representative of containments currently used for most pressurized water reactor nuclear power plants. These figures show that the area under study is complicated by the geometry and large-scale dimensions involved. The complexity is increased by manufacturing, construction, structural, aging, thermal, and accident transient considerations.

III. HEAT TRANSFER ANALYSIS

This section describes the analytical models and methods established for the analysis. Results are presented in Sec. III.C.

A. Analytical Models

The geometry for the containment liner-concrete interface under study is depicted in Figs. 1 and 2. For the purposes of analysis, the liner, anchor, and inner concrete region is represented by the two-dimensional conduction model shown in Fig. 3.⁵ The geometry represented is that of a 6.35-mm (1/4-in.) thick liner with 127-x 76.2-x 6.35-mm (5-x 3-x 1/4-in.) anchors at an interval of 0.382 m (15 in.).⁵ A one-dimensional model representation is also employed wherein the anchor is not included.

The AYER⁶ finite element heat conduction computer program was used for the thermal analyses. The following assumptions, which are representative of those currently used in Pressurized Water Reactor (PWR) dry-containment maximum pressure response analyses, were used, unless stated otherwise:

- An initial temperature of 322 K (120°F). This represents a maximum value.⁷ Appendix A (Sec. III) discusses the effect of this assumption.
- Containment atmosphere boundary condition as shown in Fig. 4.
- Thermal properties as given in Table I.⁷ Appendix A (Sec. V) discusses these properties.
- A maximum problem time of 300 s was chosen with results at 30, 100, 200, and 300 s also presented. For most containment analyses, the effect of the liner-concrete heat transfer has been asserted by 300 s.⁷

Other aspects of the heat transfer analytical models had to be determined so that adequate numerical representation was obtained. These are:

- Finite element, two-dimensional mesh as shown in Fig. 3. Note that the mesh spacing is finer near the liner and the anchor to better account for the higher temperature gradients in these regions. See Appendix A (Sec. I).
- Total concrete depth of only 0.152 m (6 in.). Concrete thicknesses of 1.143 m (3.75 ft) and 0.152 m (6 in.) were found to produce essentially identical results. See Appendix A (Sec. II).
- Problem time increments of 2 s up to 30 s and 10 s thereafter. See Appendix A (Sec. VI).

B. Method of Analysis

The containment liner-concrete heat transfer can occur by:

1. Conduction through the points of contact between the liner and the concrete.
2. Conduction across the gaps between the liner and the concrete.
3. Radiation across the gaps.
4. Natural convection in the gaps.

All these forms of heat transfer can be combined and expressed by an overall one-dimensional interface heat transfer conductance, H_c . Such a representation is convenient for use in containment pressure response analysis and will be used in the discussion below. A lower case h will be used to designate a localized interface conductance or a component of H_c . Thus, for the two-dimensional model, h_{LC} and h_{AC} represent the overall liner-concrete and anchor-concrete conductances. Also, h_k , h_r , and h_{nc} represent the conductance due to thermal conduction, radiation, and natural convection, respectively.

A major factor in the determination of the H_c for the containment liner-concrete heat transfer is the gap or liner-concrete displacement. This determines the h_k and therefore the H_c , to a great extent. It appears that the liner-concrete displacement may vary significantly throughout the containment (e.g., see Fig. 5).⁵ Section IV discusses the liner displacement in more detail. The representation of such variations for containment pressure response analyses would be awkward with currently used computer programs.² Therefore, the concept of an area-weighted mean liner-concrete displacement δ will be used in the discussion that follows. Assuming that the gap is filled with air allows δ and h_k to be related via

$$h_k = \frac{k}{\delta},$$

where k is the air thermal conductivity (see Sec. III.C.3). The effect of a variation of displacement on h_k is discussed in Sec. III.C.3.

C. Results

1. One-Dimensional Model

A convenient way to model the containment lined-concrete heat sinks is to use a one-dimensional model.² The effect of the liner-concrete interface heat transfer conductance on the energy absorbed per unit area in such a heat sink is shown in Fig. 6. Note that a 6.35mm (1/4-in.) liner is used and there is no anchor representation. The effect of the anchor will be established in the next section. Temperature distributions through the liner and concrete for the one-dimensional model are presented in Figs. 7 through 9.

The following effects are shown by these figures:

- The energy absorbed is not significantly affected by H_c at early times. As shown in Fig. 7, this is due to (a) most of the energy being absorbed in the liner and (b) the additional energy absorbed by the concrete at higher H_c corresponds to less energy storage in the liner.

- H_C has a reduced effect on E/A (absorbed energy/area) at low values and at high values of H_C . This phenomenon can be observed via Fig. 8. At low values of H_C , the primary energy storage is in the liner because of the poor thermal communication between the liner and the concrete. The energy absorbed at high values of H_C reaches a near maximum value. This is due to the inner concrete temperature reaching very nearly the maximum value possible. Since this temperature is the thermal potential for driving energy into the concrete, the energy flow into the concrete is limited.

2. Effects of Radiation, Natural Convection, and Anchors

The effect of radiation is determined in Appendix B and found to result in an equivalent h_r , for radiation only, of $\sim 5.7 \text{ W/m}^2/\text{K}$ ($1 \text{ Btu/h}\cdot\text{ft}^2\cdot^\circ\text{F}$).

Natural convection in the gaps that may exist between the liner and concrete has been investigated (see Appendix C). This analysis shows that the natural convection comes into play only for gaps $> \sim 8 \text{ mm}$ (0.3 in.) and provides a minimum conductance of $\sim 5.7 \text{ W/m}^2/\text{K}$ ($1 \text{ Btu/h}\cdot\text{ft}^2\cdot^\circ\text{F}$).

A two-dimensional representation of the containment liner, anchor, and concrete was made, as described in Sec. III.A, to study the effect of the anchors. The results of this study are presented in Fig. 10. This figure shows that:

- The anchor-concrete interface heat transfer conductance, h_{AC} , has a very small effect on E/A .
- The effect on E/A of the liner-concrete conductance, h_{LC} , is reduced at early times and at small and large values of h_{LC} . These effects are consistent with the similar observations for the one-dimensional calculations above.

An interesting result from this study is the small effect of the anchor to concrete interface conductance, h_{AC} . This is due to the following:

- At high h_{AC} , the temperature distribution within the anchor is controlled by that of the concrete with which the anchor is thermally communicating (well in this case). See Fig. 11. As a result, the energy absorbed by the anchor is limited.
- Low values of h_{AC} allow the anchor to achieve a higher temperature level but the energy addition to the concrete via the anchor is now reduced. See Fig. 12.

Figures 10 and 6 can be used to estimate the equivalent one-dimensional liner-concrete interface conductance, H_C , to represent the effect of the anchor on energy absorbed. Some examples, at 300 s, are given in Table II.

The procedure followed in Table II is:

1. Assume a liner-concrete interface conductance, e.g., $h_{LC} = 57 \text{ W/m}^2\cdot^\circ\text{F}$ ($10 \text{ Btu/h}\cdot\text{ft}^2\cdot^\circ\text{F}$). The effect of the anchor-concrete conductance h_{AC} , is shown to be negligible in Fig. 10.

2. For this, obtain the value of energy absorbed/area, E/A , at 300 s from Fig. 10, i.e., $\sim 2.89 \text{ MJ/m}^2$ (255 Btu/ft^2).
3. Obtain the equivalent one-dimensional liner-concrete conductance, H_c , that would result in this value of E/A from Fig. 6 at 300 s, i.e., $\sim 97 \text{ W/m}^2/\text{K}$ ($17 \text{ Btu/h/ft}^2/^\circ\text{F}$).

The effect of the anchor on the E/A at 300 s for the same h_{LC} is shown in the last column of Table II. For example, assume

$$h_{LC} = 57 \text{ W/m}^2/\text{K} \text{ (10 Btu/h/ft}^2/^\circ\text{F)}.$$

From Fig. 10, for this h_{LC} ,

$$(E/A)_{2D} = 2.89 \text{ MJ/m}^2 \text{ (255 Btu/ft}^2\text{)}.$$

From Fig. 6, for this h_{LC} ,

$$(E/A)_{1D} = 2.68 \text{ MJ/m}^2 \text{ (236 Btu/ft}^2\text{)}.$$

As a result, for this h_{LC} ,

$$\frac{(E/A)_{2D}}{(E/A)_{1D}} = 1.08.$$

The variation of this ratio with h_{LC} as shown in Table II indicates that the effect of the anchors decreases as the h_{LC} increases. This trend will be the same at smaller times except that the magnitudes of the ratio will be reduced. See Table III.

An alternate simplified means of representing the anchors is to use two one-dimensional models; one consisting of the liner and concrete, and the other having the anchor and concrete. This method was analyzed for a 0.127-m (5-in.)-long anchor with an interface conductance between the anchor and concrete of $\sim 57 \text{ W/m}^2/\text{K}$ ($10 \text{ Btu/h/ft}^2/^\circ\text{F}$). An (E/A) at 300 s of 8.25 MJ/m^2 (727 Btu/ft^2) resulted. The one-dimensional liner concrete model has been analyzed, Fig. 6. For the same conductance, $(E/A)_{300 \text{ s}} = 2.61 \text{ MJ/m}^2$ (230 Btu/ft^2). An area-weighted $(E/A)_{300 \text{ s}}$ can now be calculated based on the area fractions of 0.0167 for the anchor-concrete only and 0.9833 for the liner-concrete only models, Fig. 3. A

value of 2.70 MJ/m^2 (238 Btu/ft^2) results. This can be compared to a value of 2.87 MJ/ft^2 (253 Btu/ft^2) from Fig. 10 wherein the anchor has been accounted for by the two-dimensional model.

3. Liner-Concrete Conductance vs Gap

The liner-concrete interface conductance can be readily expressed in terms of an equivalent air gap, or vice versa. This relationship is shown in Fig. 13 for an air thermal conductivity at 373 K (212°F), see Table IV. Also shown on this figure are:

- An approximate line-thickness representation for various gap thickness. This is done to provide an appreciation for the gap size.
- The additional effect of the gap radiation assumed to be $\sim 5.7 \text{ W/m}^2/\text{K}$ ($1 \text{ Btu/h/ft}^2/^\circ\text{F}$) as calculated in Appendix B.

Figure 13 allows the ready estimation of the equivalent gap conductance due to conduction and radiation from any given area-mean liner-concrete gap.

4. Effect of Displacement Variation

The concept of using an area-weighted mean liner-concrete displacement to represent a variable displacement was investigated. The two-dimensional model of Fig. 3 without anchors was used. A linear variation of the displacement between the liner and concrete along a span of 0.38 m (15 in.) was assumed. The resulting absorbed energy can then be compared with the energy for an assumed constant displacement equal to the area-weighted average of the variation. Results are summarized in Table V for two cases. In each case, the local displacement is used to find a local interface conductance from Fig. 13. Thus, a displacement of 0.0254 mm (0.001 in.) corresponds to a value of $h_{LC} = 625 \text{ W/m}^2/\text{K}$ ($110 \text{ Btu/h/ft}^2/^\circ\text{F}$) and a displacement of 1.04 mm (0.041 in.) corresponds to a value of $h_{LC} = 34 \text{ W/m}^2/\text{K}$ ($6 \text{ Btu/h/ft}^2/^\circ\text{F}$), etc. The h_{LC} will vary inversely with the displacement. For this case the area-weighted mean-displacement is 0.533 mm (0.021 in.), which corresponds to an $h_{LC} = 61 \text{ W/m}^2/\text{K}$ ($11 \text{ Btu/h/ft}^2/^\circ\text{F}$). Table V shows that the energy absorbed/area at 300 s is 2.84 MJ/m^2 ($250 \text{ Btu/h/ft}^2/^\circ\text{F}$) with this linear variation of the displacement. Using the area-weighted mean-displacement for this case results in an E/A at 300 s of 2.67 MJ/m^2 ($235 \text{ Btu/h/ft}^2/^\circ\text{F}$), a difference of 6%.

The comparisons of Table V show that the use of a mean-displacement can produce absorbed energies within $\sim 10\%$ of the result based on the actual displacement. However, large variations of the displacement could be better represented by several constant displacement models. Note that the results of Table V

indicate that the use of an area-weighted mean-displacement results in less energy absorbed.

5. Combined Effects on Energy Absorbed and on One-Dimensional Liner-Concrete Conductance

This section will show and discuss the combined effects of the various heat transfer modes on the (a) energy absorbed after 300 s, Fig. 14, and (b) one-dimensional liner-concrete conductance, Fig. 15. Figure 14 shows the following influences of the various effects on the energy absorbed after 300 s:

1. Liner-concrete gaps in the range of 0.01 to 1 mm (0.0004 to 0.04 in.) have a significant influence ($\pm 20\%$) on the energy absorbed.
2. Gaps smaller than the range specified in (1) have a small effect because conduction into the concrete is the limiting resistance to energy absorption.
3. Gaps larger than the range specified in (1) have a small effect because heat transfer across the gap is primarily by radiation and secondarily by natural convection.
4. The anchors have a larger effect ($\sim 10\%$) at larger gap sizes because of the poor thermal communication between the liner and the concrete.

The various heat transfer effects on the one-dimensional interface heat transfer conductance, H_C , are shown in Fig. 15. This figure shows that:

1. H_C reaches a minimum value of $\sim 57 \text{ W/m}^2/\text{K}$ ($10 \text{ Btu/h/ft}^2/^\circ\text{F}$) at gap sizes larger than $\sim 2.54 \text{ mm}$ (0.1 in.).
2. The effects of radiation and natural convection become insignificant for gap sizes smaller than $\sim 1 \text{ mm}$ (0.04 in.).
3. A value of H_C greater than $\sim 2800 \text{ W/m}^2/\text{K}$ ($500 \text{ Btu/h/ft}^2/^\circ\text{F}$) would result in approximately the maximum energy absorbed at 300 s. See Fig. 14.

IV. LINER DISPLACEMENT CONSIDERATIONS

The heat transfer analyses above show the importance of the area-mean displacement or gap between the liner and the concrete on the energy absorbed. The problem then becomes a matter of determining this value.

To develop an appreciation for the nature of the displacement, the literature regarding lined concrete containment and reactor vessels was reviewed.^{3-5,8,9} This review indicates that the following factors will affect the geometry of the liner-concrete displacement under transient accident LOCA conditions, i.e.,

increasing containment internal temperature and pressure:

1. Initial curvature of the liner plate.⁵
2. Inward radial movement of the concrete shell due to prestressing, concrete shrinkage, and creep with aging.⁴
3. Variation of anchor spacing.⁵
4. Variation in plate thickness, e.g., +16%, -4%.⁵
5. Variation in liner yield stress.⁹
6. Variation of Poisson's ratio and modulus of elasticity of the liner plate.⁵
7. Variation of concrete modulus of elasticity and anchor stiffness.⁵
8. Cracking or crushing of concrete in the local liner plate anchorage zone.⁵
9. Tolerances of the liner plate and anchorage system, e.g., anchor spacing is $\pm 1/8$ in.⁵
10. Containment internal pressure.
11. Liner and concrete temperature.
12. Plate stresses exceeding the yield stress with the possibility of buckling.⁴
13. Evolution of steam from the concrete causing a pressure build-up between the concrete and the liner.⁸

In addition to the above considerations, the geometry of the displacement is multidimensional, as shown in Fig. 5, and is different, generally speaking, for the cylindrical and the dome liners.

In view of the above, it is apparent that the prediction of the transient liner-concrete displacement over the complete containment liner-concrete interface is far from simple. Statistical structural analyses, with all variations and permutations considered, or experimental investigations are required to quantify the displacement. The resulting area-weighted mean liner-concrete displacement could then be applied to the heat transfer analysis results, presented herein, to establish containment liner-concrete interface conductances.

V. EFFECT ON CONTAINMENT PRESSURE

The basic objective of this report is to determine the effect of various complexities such as anchors and radiation on the liner-concrete heat transfer. One of the main applications of such an analysis is the determination of the energy absorbed by lined-concrete structures in containment pressure response

analyses. The energy absorbed affects the energy remaining in the containment which, in turn, affects the containment pressure. In fact, the pressure (P) is approximately proportional to the containment atmosphere energy (E_c).¹⁰ In equation form,

$$P \propto E_c$$

and

$$\frac{dP}{P} = \frac{dE_c}{E_c} \quad (1)$$

From the first law of thermodynamics, the energy in the containment is given as

$$E_c = E_{\text{initial}} + E_{\text{added}} - E_{\text{lost}} \cdot$$

The energy lost term is composed of the energy transferred to the liner-concrete heat sink (E_{LC}) and other losses. At a given time, the initial energy, added energy, and other energy losses can be assumed constant, resulting in

$$dE_c = dE_{LC} \quad (2)$$

Some representative values can now be substituted into the above equations. The total energy in the containment at the time of peak pressure is^{10,11}

$$E_c \approx 0.4 \text{ to } 0.5 \text{ TJ } (4 \text{ to } 5 \times 10^8 \text{ Btu}) \cdot$$

The total lined-concrete heat sink area is^{10,11}

$$A_{LC} \approx 10^4 \text{ m}^2 (10^5 \text{ ft}^2) \cdot$$

From Fig. 10, the energy absorbed/area at 300 s can vary between

$$(E/A)_{LC} \approx 2.3 \text{ to } 4.0 \text{ MJ/m}^2 (200 \text{ to } 350 \text{ Btu/ft}^2) \cdot$$

Multiplication of the $(E/A)_{LC}$ by the A_{LC} gives,

$$E_{LC} \approx 0.02 \text{ to } 0.04 \text{ TJ } (0.2 \text{ to } 0.35 \times 10^8 \text{ Btu}).$$

Therefore,

$$E_{LC} \approx 0.04 \text{ to } 0.1 E_c . \quad (3)$$

Substituting Eqs. (2) and (3) into Eq. (1) results in

$$\frac{dP}{P} \approx 0.04 \text{ to } 0.1 \frac{dE_{LC}}{E_{LC}} . \quad (4)$$

On the basis of Eq. (4), a 20% change in the lined-concrete energy absorption could result in a 1-2% change in calculated pressure. For example, a containment design pressure of 0.3 to 0.4 MPa (50 to 60 psi) could be affected by 3-7 kPa (0.5 to 1 psi) based on the above development. This is an approximate result and depends on the assumptions made. However, the above development might be used to approximate the significance of changes in the $(E/A)_{LC}$.

VI. CONCLUSIONS

Conclusions derived from the containment liner-concrete interface heat transfer analyses of this report are now presented. These conclusions should be utilized with a clear understanding of their technical base. In particular, the general model assumptions presented in Sec. III.A should be understood.

The conclusions are:

1. Thermal radiation across the liner-concrete interface is equivalent to a conductance of $\sim 5.7 \text{ W/m}^2/\text{K}$ ($1 \text{ Btu/h}\cdot\text{ft}^2\cdot^\circ\text{F}$). See Appendix B.
2. The effect of the anchors on the energy absorbed has been investigated for a representative anchor design. For example, after 300 s, with a liner-concrete conductance of $57 \text{ W/m}^2/\text{K}$ ($10 \text{ Btu/h}\cdot\text{ft}^2\cdot^\circ\text{F}$), the anchors increase the energy per unit area absorbed by $\sim 8\%$. See Sec. III.C.2. This conclusion depends on the anchor design used and could be different for other geometries.
3. Natural convection makes a conductance contribution of $\sim 5.7 \text{ W/m}^2/\text{K}$ ($1 \text{ Btu/h}\cdot\text{ft}^2\cdot^\circ\text{F}$) if large gaps greater than 7.6 mm (0.3 in.) should occur. Gaps smaller than this would result in conductances based on simple conduction across a gap.

4. The effect of contact and gap conduction on the liner-concrete interface heat transfer requires knowledge of the spatial distribution of the liner-concrete displacement or gap.
5. Determination of the gap distribution requires extensive structural analyses, or experiments to account for the many variations and permutations inherent in the liner-concrete structural system, especially under accident conditions.
6. Multidimensional liner-concrete interface heat transfer can be approximately represented by an equivalent one-dimensional conductance, H_c , for transient pressure response analyses.
7. A reasonable minimum value for H_c is $\sim 57 \text{ W/m}^2/\text{K}$ ($10 \text{ Btu/h/ft}^2/^\circ\text{F}$). See Sec. III.C.5, Fig. 15.
8. A variation of H_c from 28 to $85 \text{ W/m}^2/\text{K}$ (5 to $15 \text{ Btu/h/ft}^2/^\circ\text{F}$) results in an approximate $\pm 10\%$ variation in the energy absorbed, Fig. 6. The resulting effect on containment maximum pressure is $\sim \pm 1\%$. See Sec. V.
9. A reasonable maximum value for H_c is $\sim 2800 \text{ W/m}^2/\text{K}$ ($500 \text{ Btu/h/ft}^2/^\circ\text{F}$) on the basis that this would result in a one-dimensional energy absorbed at 300 s (Fig. 6), within $\sim 5\%$ of the maximum potential energy absorbed.

ACKNOWLEDGMENT

T. J. Merson (WX-8, LASL) provided valuable assistance in this study by performing most of the calculations, as well as reviewing the basic technical content.

APPENDIX A
MODEL DEFINITION

I. MESH SPACING

Numerical representation of a geometry must include an evaluation to determine that adequately fine increments are used. All calculations of this report are based on the mesh spacing shown in Fig. 3. The one-dimensional model uses this incrementation in the direction normal to the liner with the effect of the anchor leg excluded. The concrete finite element mesh spacing in the direction normal to the liner is approximately

$$\Delta y_1 = 1.3 \text{ mm (0.05 in.)}$$

$$\Delta y_2 = 2.5 \text{ mm (0.1 in.)}$$

$$\Delta y_3 = 3.8 \text{ mm (0.15 in.)}$$

.

.

.

etc.

The adequacy of this y-direction mesh spacing was checked via the two-dimensional model with the results summarized in Table A-I. This comparison shows that the total energy absorbed varies by only ~ 2% for this major variation, thereby indicating that the finer mesh spacing is adequate. Another check was made with the one-dimensional model using the graduated mesh spacing, i.e., Δy_1 , $\Delta y_2 = 2\Delta y_1$, $\Delta y_3 = 3\Delta y_1$, etc., but with various Δy_1 . The results of this study are summarized in Table A-II. Again, the mesh spacing used is shown to be adequate.

Further verification that the y-direction mesh spacing used in this analysis is adequate is provided in Ref. 12. This reference indicates that a criterion that can be used is

$$\Delta y < 0.3 \sqrt{\alpha \theta} ,$$

where

$$\alpha = \text{thermal diffusivity, m}^2/\text{s (ft}^2/\text{h)} ,$$

θ = time from start, s (h), and

Δy = mesh spacing, m (ft).

In particular, for concrete,

$$\alpha \approx 7.7 \times 10^{-7} \text{ m}^2/\text{s} \text{ (0.03 ft}^2/\text{h)}$$

with

$\theta = 300 \text{ s (0.084 h), and}$

$\Delta y < 4.6 \text{ mm (0.015 ft} \approx 0.18 \text{ in.)}$.

The finite element mesh spacing in the x-direction (i.e., parallel to the liner) was also studied. This spacing was varied from a constant value of 0.8 mm (0.03 in.) to a graduated series, proceeding from the liner of approximately 0.08, 0.15, 0.23, etc. mm (0.003, 0.006, 0.009, etc., in.). See Fig. 3. This variation resulted in only $\sim 0.1\%$ difference in the total energy absorbed after 300 s. This small effect is due to the relatively small temperature gradients in this direction, see Figs. 11 and 12.

II. CONCRETE DEPTH

The liner-concrete heat transfer models (e.g., Fig. 3) include a representation of the containment concrete, which can be as much as $\sim 1.2 \text{ m (4 ft)}$ thick (Fig. 1). This could require a large number of elements in a numerical representation of the concrete, which would result in large computer storage and running times.

Two-dimensional model problems with concrete thicknesses of 1.14 and 0.15 m (3.75 and 0.5 ft) with corresponding numbers of nodal points of 1337 and 950, respectively, were calculated. Interface conductances of $570 \text{ W/m}^2/\text{K}$ ($100 \text{ Btu/h/ft}^2/^\circ\text{F}$) were used at the liner-concrete and anchor-concrete interfaces. The net energies absorbed, after 150 s for the two cases, were identical within six significant figures. This result is readily appreciated from the temperature distributions shown in Figs. 7 through 9 and Figs. 11 and 12.

As a result, all calculations discussed in this report utilized a concrete thickness of 0.15 m (6 in.).

III. INITIAL TEMPERATURE

An initial temperature or temperature distribution for the liner-concrete models must be assumed. A uniform value of 322 K (120°F) was chosen because this is a currently used assumption for maximum containment pressure-temperature response analysis.⁷ However, different values might be of interest. Toward this end, Fig. A-1 shows the effect of the initial temperature on the energy absorbed. Note the interface conductances used. In particular, a lower value for the liner-concrete contact coefficient, h_{LC} , would reduce the effect of the initial temperature while a higher value for h_{LC} would increase the effect of the initial temperature.

Values of energy absorbed in Fig. A-1 are slightly different from those presented in Fig. 10 for an initial temperature of 120°F because of the different containment atmosphere boundary conditions used. Figure 10 is based on the boundary conditions of Fig. 4. See the following section.

IV. ATMOSPHERE BOUNDARY CONDITIONS

The basic containment boundary conditions used for the various analyses were specified to be those representative of that used in containment maximum pressure response analyses. These are shown in Fig. 4. Calculations were also performed with a more simple boundary condition of

$$h_{atm} = 568 \text{ W/m}^2/\text{K} \text{ (100 Btu/h/ft}^2/\text{°F)}$$

$$T_{atm} = 400 \text{ K (260° F)} .$$

A comparison of these boundary conditions with those given on Fig. 4 reveals that comparable results should be obtained from the use of either set of boundary conditions.

Figure A-2 shows the energy absorbed per unit area for the two boundary conditions. A maximum difference of ~ 7% is indicated. At later times, the two cases produce nearly the same E/A because the major time portion of the Fig. 4 boundary condition is essentially the same as the simple boundary condition. At early times the heat sink thermal inertia reduces the influence of the boundary condition. Figure A-2 also shows the energy distribution between the model components, i.e., liner, concrete, and anchor.

For the two boundary conditions, Fig. A-3 compares the instantaneous atmosphere to liner heat fluxes, for the two boundary conditions, defined as

$$\dot{E}/A = \sum_i \frac{\dot{E}_i A_i}{A},$$

where

\dot{E}/A = average atmosphere-to-liner heat flux,

\dot{E}_i = average atmosphere-to-liner energy rate over increment i in the numerical representation of the liner (see Fig. 3),

A_i = increment i area, and

A = total liner area in the numerical representation, i.e., $\sum_i A_i$.

Figure A-3 indicates that the heat flux variations are quite comparable for the two boundary conditions, after 30 s, as would be expected.

V. CONCRETE PROPERTIES

The liner, anchor, and concrete properties (Table I) used in the analysis represent values commonly used in containment maximum pressure-temperature response analyses.⁷ The steel properties are quite standard and will not be discussed further.

Reference 9 gives concrete property information with a minimum thermal conductivity (k) of ~ 1.4 W/m/K (0.8 Btu/h/ft/ $^{\circ}$ F). This same reference indicates a maximum value for the diffusivity (α) of 6.2×10^{-7} m²/s (0.024 ft²/h) for this k . For a density (ρ) of 2082 kg/m³ (130 lbm/ft³), a value of specific heat (c) of ~ 1090 J/kg/K (0.26 Btu/lbm/ $^{\circ}$ F) results. This value of c is within $\sim 10\%$ of the value used in these analyses.

A simple check of the effect of a variation of α was made by running a one-dimensional analysis with $H_c = 63$ w/m²/K (11 Btu/h/ft²/ $^{\circ}$ F), the same k and ρ above, and a $c = 2390$ J/kg/K (0.57 Btu/lbm/ $^{\circ}$ F). This value for c corresponds to the minimum value of $\alpha = 2.8 \times 10^{-7}$ m²/s lbm (0.011 ft²/h) indicated by Ref. 9 for $k = 1.4$ w/m/K (0.8 Btu/h/ft/ $^{\circ}$ F). The resulting energy absorbed at 300 s was 26% higher than with the higher α .

VI. TIME INCREMENT

Numerical transient analyses such as those presented in this report require that the transient time increment, Δt , be varied to assure that an adequately small value for Δt is used. The results of such a time increment selection check are summarized in Table A-III. This table shows that the Δt used are adequate.

They are

$$\Delta t = 2 \text{ s to } 30 \text{ s}$$

and

$$\Delta t = 10 \text{ s after } 30 \text{ s .}$$

The variation of the Δt with time is based on the boundary condition variation being more severe up to 30 s (see Fig. 4).

APPENDIX B

EFFECT OF RADIATION ON LINER-CONCRETE HEAT TRANSFER CONDUCTANCE

The radiation between the liner and the concrete is essentially that for radiation between infinite parallel plates. For this case,¹³

$$q = \frac{\sigma(T_1^4 - T_2^4)}{\frac{1}{E_1} + \frac{1}{E_2} - 1} ,$$

where

q q = energy rate per unit area,

σ σ = Stefan-Boltzmann constant,

T_1, T_2 = surface temperatures, and

E_1, E_2 = surface emissivities.

Equating this energy rate with an expression involving an equivalent radiation interface conductance, h_r , gives,

$$q = h_r (T_1 - T_2) = \frac{\sigma(T_1^2 + T_2^2)(T_1 + T_2)(T_1 - T_2)}{\frac{1}{E_1} + \frac{1}{E_2} - 1} .$$

Thus,

$$h_r = \frac{\sigma(T_1^2 + T_2^2)(T_1 + T_2)}{\frac{1}{E_1} + \frac{1}{E_2} - 1} .$$

To provide a minimum h_r , suitably low values for the emissivities are approximately ¹⁴

Steel = 0.6

and

Concrete = 0.6 .

For the problem at hand, the range of temperatures is 322 to 400 K (120 to 260°F). Substituting these values gives,

for $T_1 = T_2 = 322$ K (120°F \equiv 580°R);

$$h_r = 3.4 \text{ w/m}^2/\text{K} \text{ (0.6 Btu/h/ft}^2/\text{°F)} ;$$

for $T_1 = T_2 = 400$ K (260°F \equiv 740°R);

$$h_r = 6.3 \text{ w/m}^2/\text{K} \text{ (1.1 Btu/h/ft}^2/\text{°F)} .$$

The radiation heat transfer was also programmed into the one-dimensional calculational model and found to be $\sim 4.5 \text{ W/m}^2/\text{K}$ ($0.8 \text{ Btu/h/ft}^2/\text{°F}$) for most of the 300 s transient, particularly after the initial ~ 30 s.

One can conclude, then, that the radiation contribution to the heat transfer across the containment liner-concrete interface can be expressed as a component of the overall conductance with a value of $h_r \sim 5.7 \text{ w/m}^2/\text{K}$ ($1 \text{ Btu/h/ft}^2/\text{°F}$).

APPENDIX C

EFFECT OF NATURAL CONVECTION ON THE LINER-CONCRETE HEAT TRANSFER CONDUCTANCE

Natural convection heat transfer across vertical enclosed air spaces can be expressed by, ¹⁵

$$\frac{h_{nc} t}{k} = \frac{C}{(L/t)^{1/9}} (N_{Gr} N_{Pr})^{1/n},$$

where

h_{nc} = natural convection heat transfer coefficient,

t = enclosed air space clearance,

k = thermal conductivity of fluid,

L = vertical length,

C = constant (see discussion below),

N_{Gr} = Grashof number (see below),

N_{Pr} = Prandtl number (see below), and

n = constant (see below).

The value of N_{Pr} for air is approximately 0.7. The Grashof number is defined as

$$N_{Gr} = \frac{t^3 \rho^2 g \beta \Delta T}{\mu^2},$$

where

ρ = fluid density,

g = acceleration due to gravity, i.e., 9.81 m/s² (4.17 x 10⁸ ft/h²),

β = coefficient of volumetric expansion = 1/T for a perfect gas where T is the absolute temperature,

ΔT = temperature potential, and

μ = fluid viscosity.

The values of C and n depend on N_{Gr} as follows:

- $N_{Gr} < 2 \times 10^3$ natural convection is suppressed and conduction controls, i.e., $h = k/t$
- $2 \times 10^3 < N_{Gr} < 2 \times 10^4$, $C = 0.2$ and $n = 1/4$
- $2.1 \times 10^5 < N_{Gr} < 1.1 \times 10^7$, $C = 0.071$ and $n = 1/3$.

For air at atmospheric pressure and 361 K (190°F),

$$N_{Gr} N_{Pr} = 8.6 \times 10^5 t^3 \Delta T.$$

For $\Delta T = 311$ K (100°F), the effect of t is

t			$N_{Gr} (N_{Pr} = 0.7)$
mm	in.	ft	
0.025	0.001	8.3×10^{-5}	$\ll 1$
0.25	0.010	8.3×10^{-4}	0.07
2.5	0.1	8.3×10^{-3}	71
5.1	0.2	0.017	569
7.6	0.3	0.025	1920

Thus, an enclosed air-space gap of ~ 7.6 mm (~ 0.3 in.) or more is required to obtain $N_{Gr} > 2\,000$ so that natural convection will make an additional contribution to the liner-concrete heat transfer. Table C-I shows the results of natural convection calculations with various gap thicknesses. Note that a minimum liner-concrete interface conductance of 3.4 to 12 $W/m^2/K$ (0.6 to 2 $Btu/h/ft^2/^\circ F$) results with gaps 2.5 mm (0.1 in.) or greater. This is due to the natural convection becoming more effective for the large gap size.

REFERENCES

1. "Standard Review Plan for the Review of Safety Analysis Reports for Nuclear Power Plants," U.S. Nuclear Regulatory Commission, Office of Nuclear Reactor Regulation report NUREG-75/087, LWR edition (September 1975).
2. L. L. Wheat, R. J. Wagner, G. F. Niederauer, C. F. Obenchain, "CONTEMPT-LT: A Computer Program for Predicting Containment Pressure-Temperature Response to a Loss-of-Coolant-Accident," Aerojet Nuclear Company report ANCR-1219 (1975).
3. "Prestressed Concrete Nuclear Reactor Containment Structures," Bechtel Corporation report BC-TOP-5-A, Revision 3 (February 1975).
4. C. P. Tan, "A Study of the Design and Construction Practices of Prestressed Concrete and Reinforced Concrete Containment Vessels," The Franklin Institute Research Laboratories report F-C2121, TID-25176 (August 1969).
5. "Containment Building Liner Plate Design Report," Bechtel Corporation report BC-TOP-1, Revision 1 (December 1972).
6. R. G. Lawton, "The AYER Heat Conduction Computer Program," Los Alamos Scientific Laboratory report LA-5613-MS (May 1974).
7. R. W. Braddy and J. W. Theising, "Performance and Sizing of Dry Pressure Containments," Bechtel Power Corporation report BN-TOP-3, Revision 3 (August 1975).

8. L. M. Polentz, "Analyses of Steel Liners on Concrete Structures," Hanford Engineering Development Laboratory report HEDL-TC-274 (Draft of HEDL-TME-75-59) (June 1975).
9. C. P. Tan, "Prestressed Concrete in Nuclear Pressure Vessels--A Critical Review of Current Literature," Oak Ridge National Laboratory report ORNL-4227 (May 1968).
10. K. D. Schwartzrauber and M. P. Pervich, "Performance and Sizing of Dry Pressure Containments," Bechtel Corporation report BN-TOP-3 (December 1972).
11. R. C. Mitchell, "Description of the CONTRANS Digital Computer Code for Containment Pressure and Temperature Transient Analysis," Combustion Engineering report CENDP-140-A (June 1976).
12. A. M. Clausing, "Practical Techniques for Estimating the Accuracy of Finite Difference Solutions to Parabolic Equations," ASME Paper No. 72-WA/APM-12.
13. J. R. Howell and R. Siegel, "Thermal Radiation Heat Transfer, Vol. II -- Radiation Exchange Between Surfaces and in Enclosures," National Aeronautics and Space Administration report NASA SP-164 (1969).
14. G. G. Gubareff, J. E. Janssen, and R. H. Torborg, "Thermal Radiation Properties Survey," Honeywell Research Center report (1960).
15. W. H. McAdams, Heat Transmission (McGraw-Hill, NY, 1954).

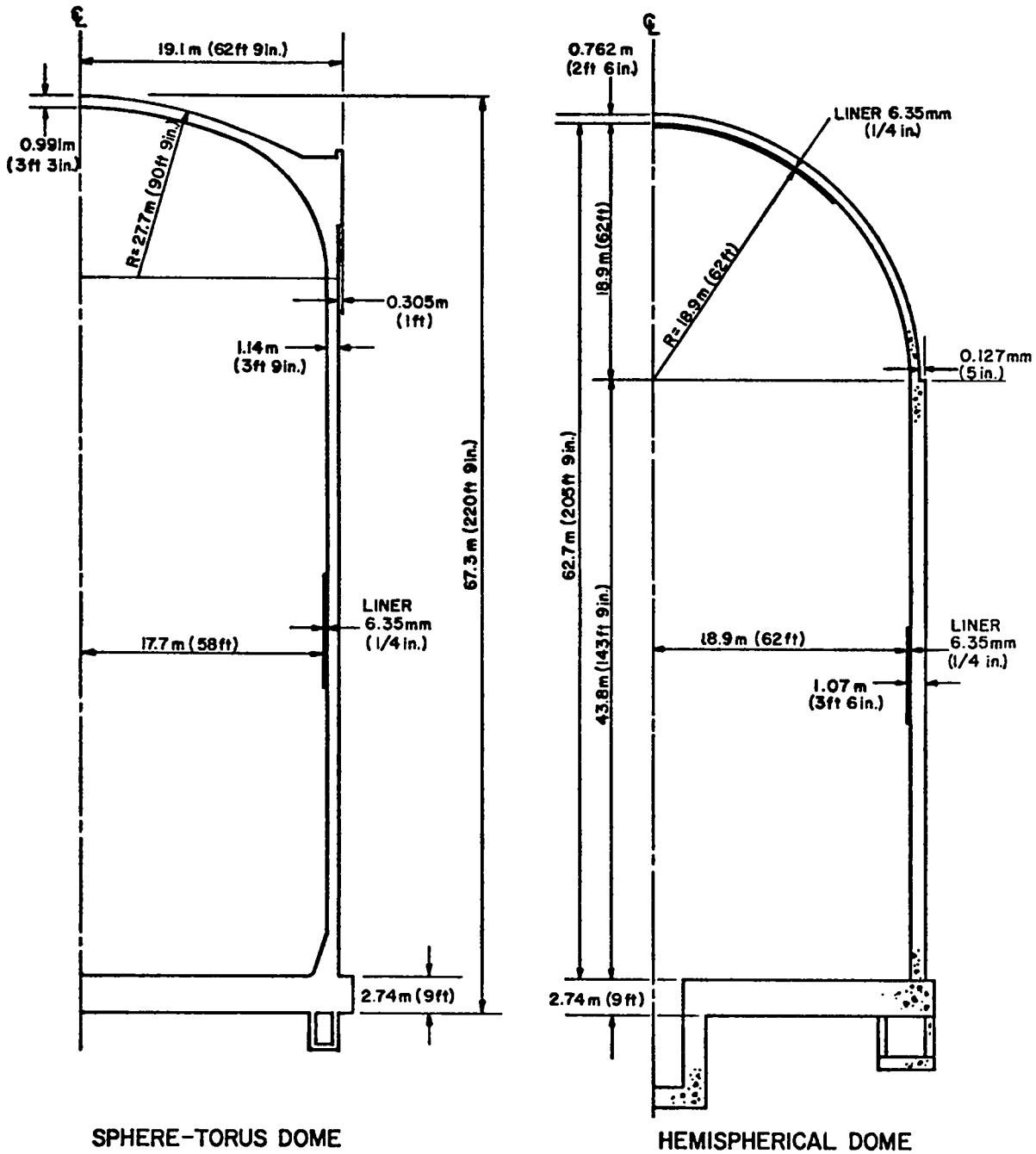


Fig. 1. Typical dry-containment configuration (Ref. 3).

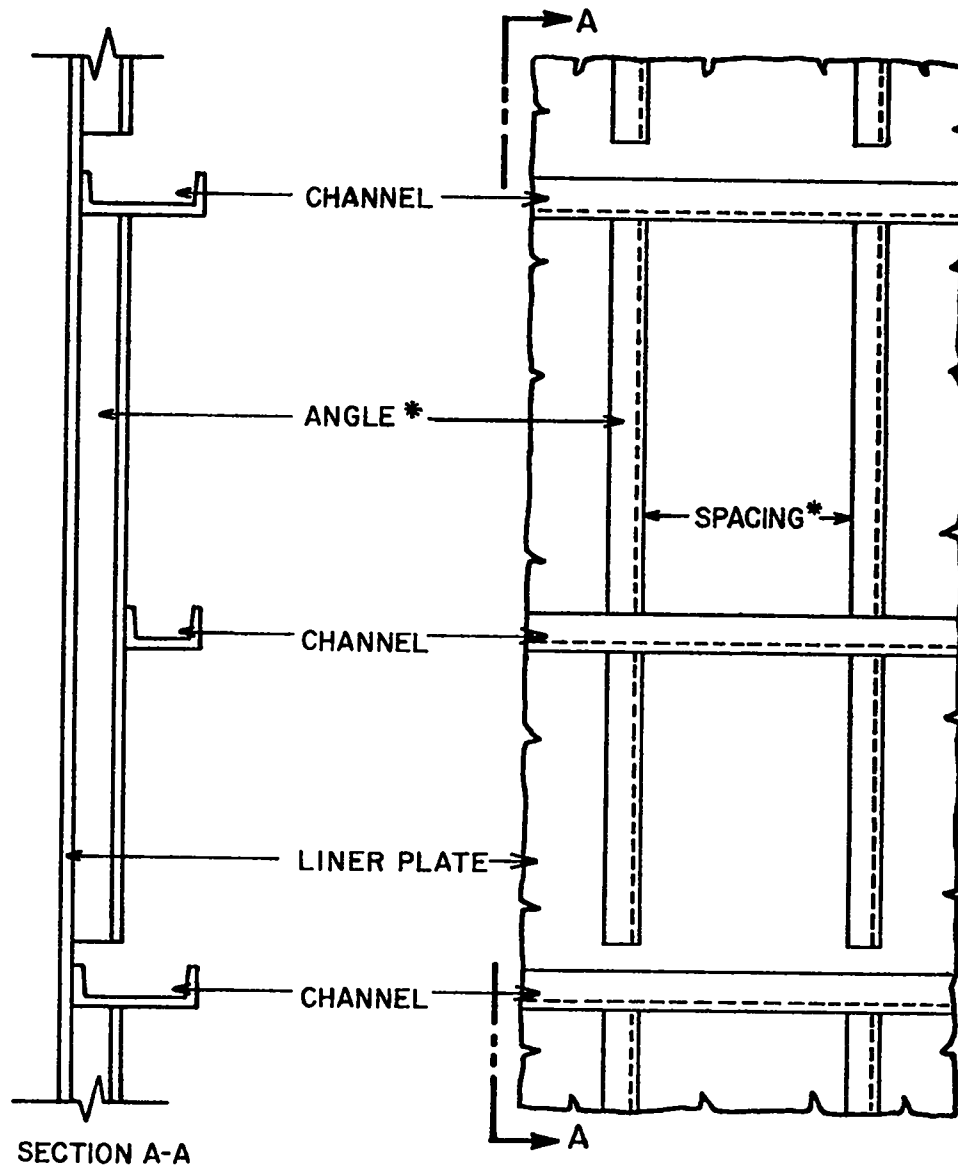


Fig. 2. Prestressed concrete containment vessel liner (Ref. 4).

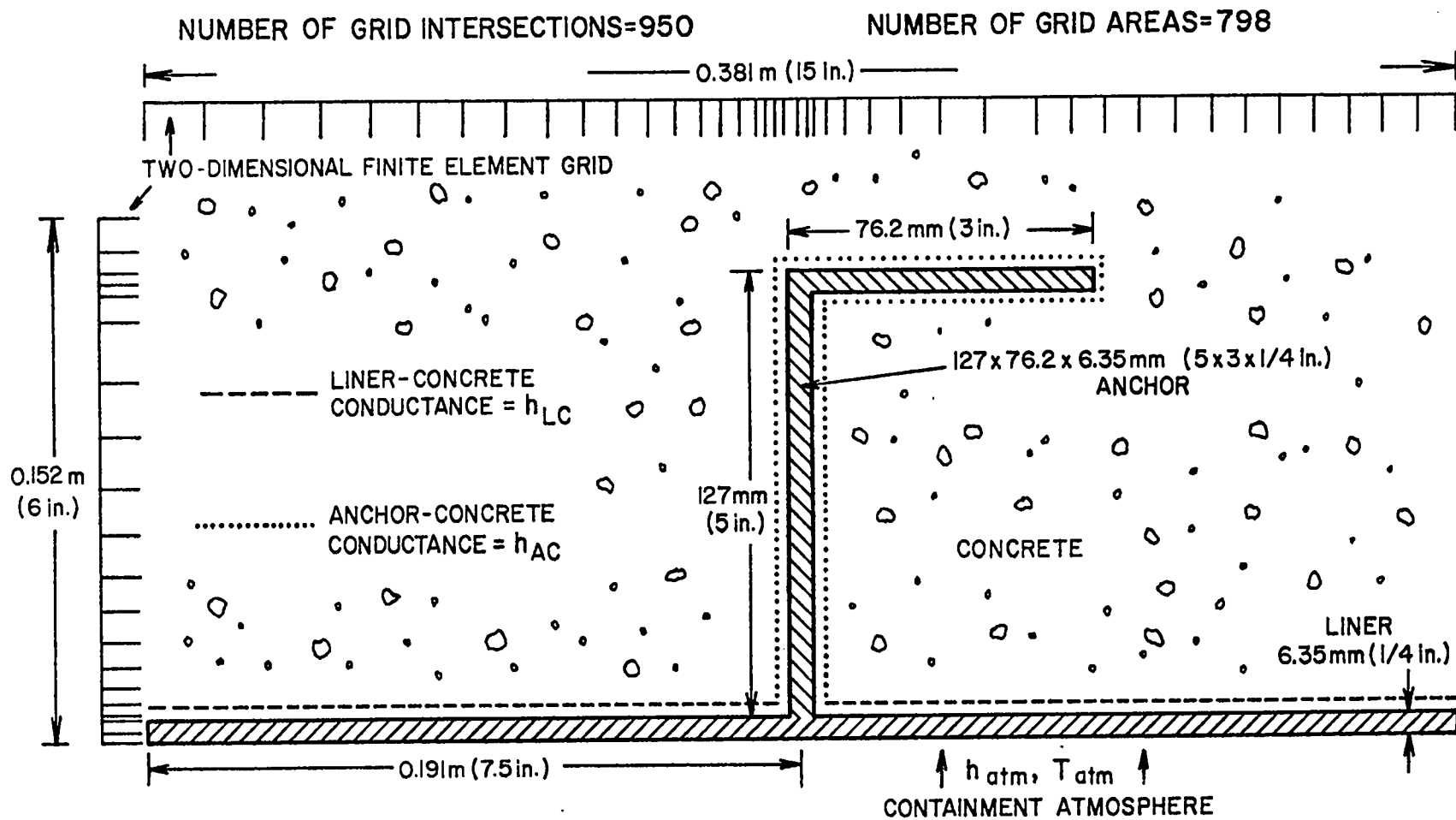


Fig. 3. Two-dimensional analytical model of a representative containment liner, anchor, and concrete region.

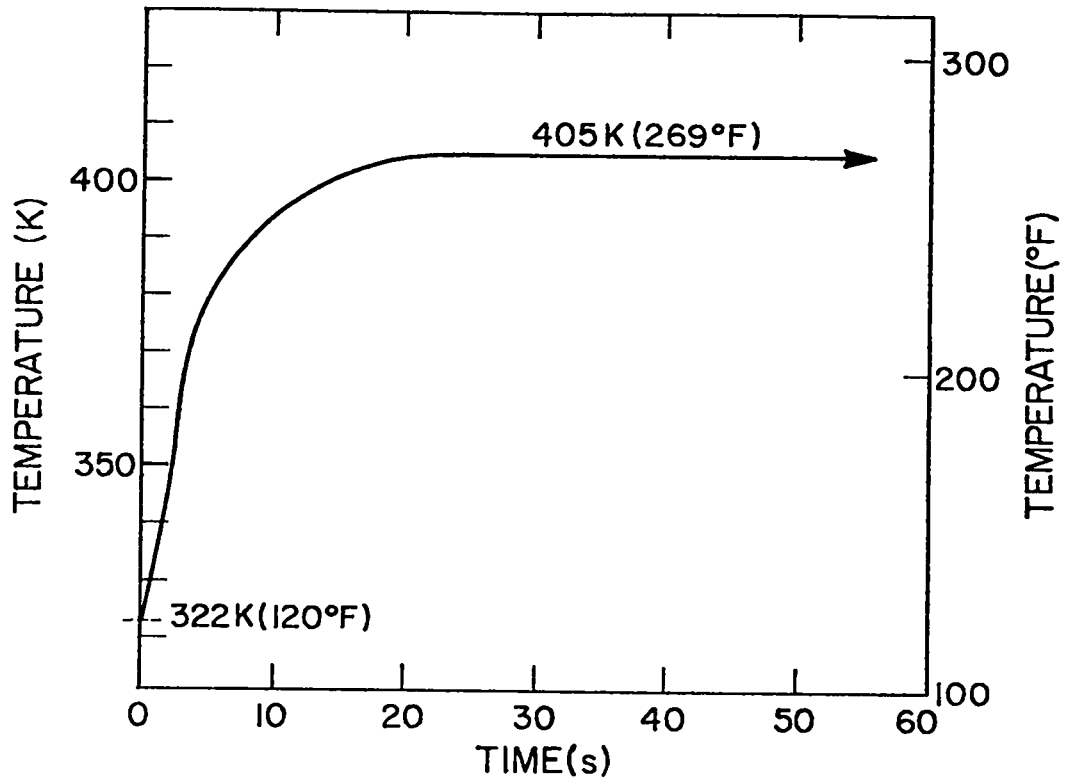
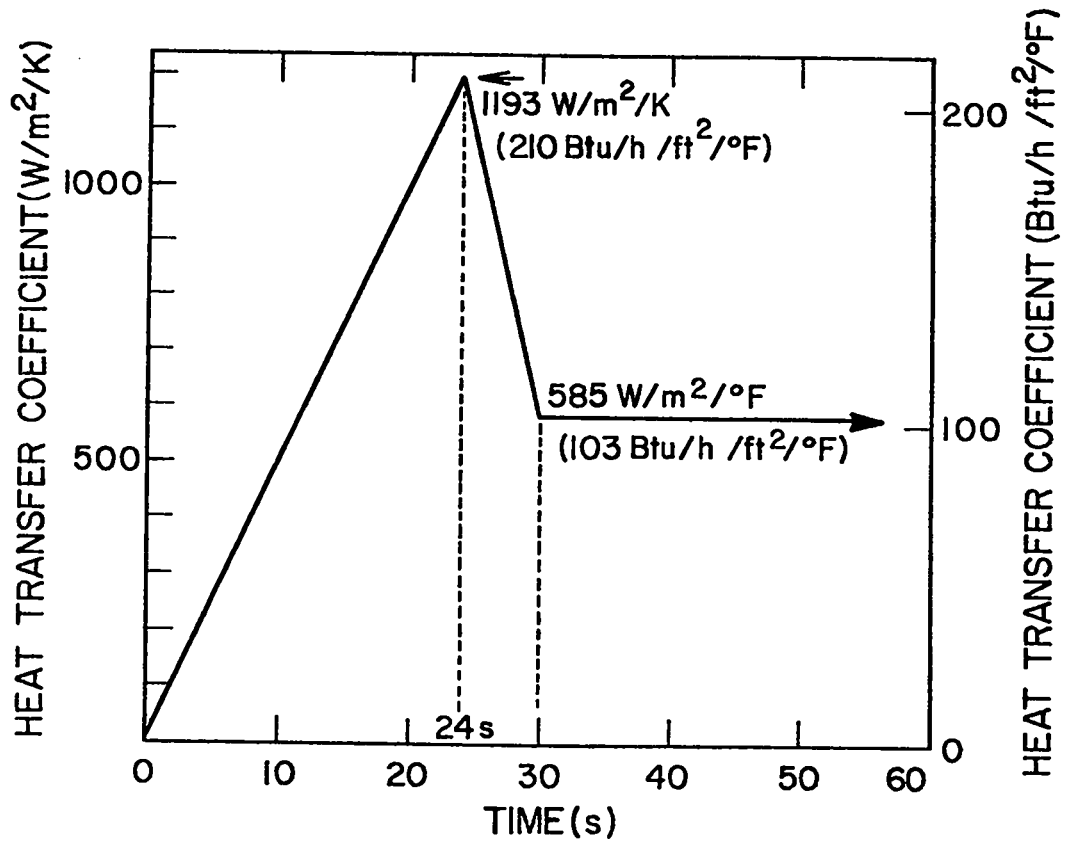
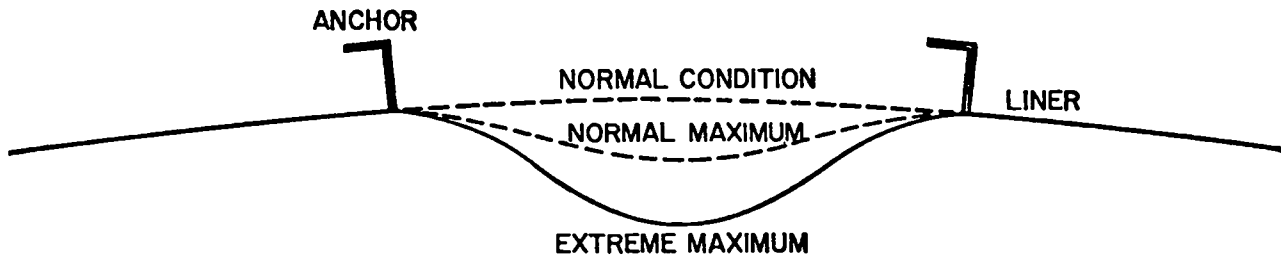


Fig. 4. Containment atmosphere boundary conditions.



NORMAL MAXIMUM LINER-CONCRETE DISPLACEMENT IS $\sim 1.59-3.18\text{mm}$ (1/16-1/8 in.)

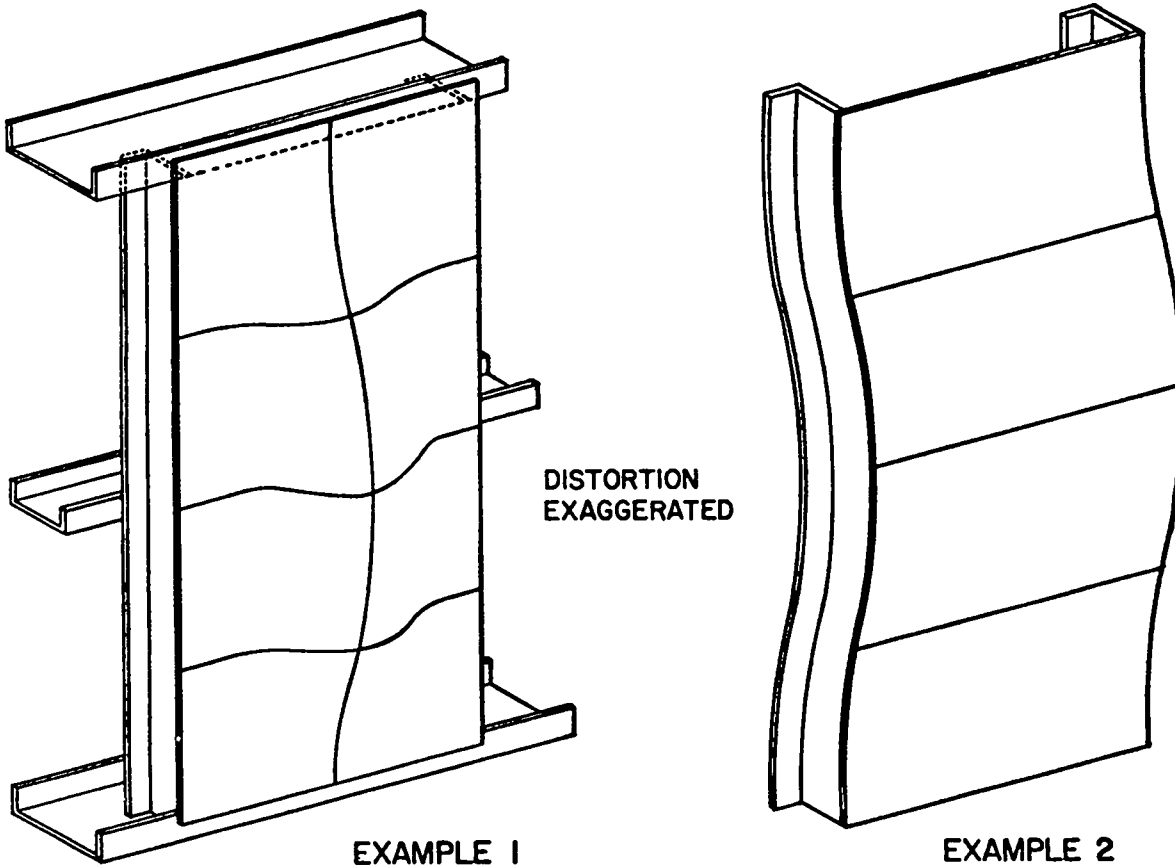


Fig. 5. Examples of extreme variations of liner-concrete displacements (Ref. 5).

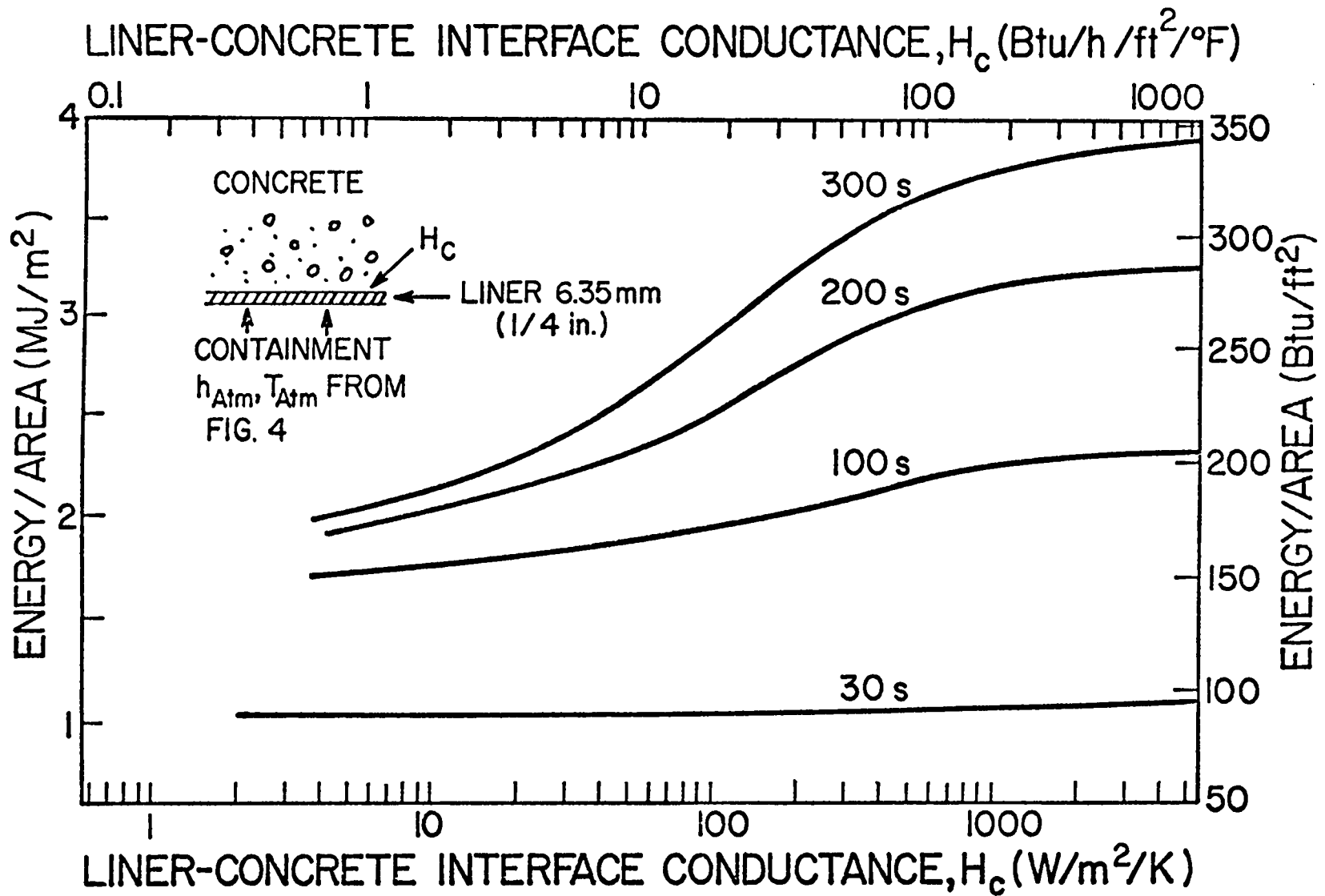


Fig. 6. Effect of H_c on energy/area absorbed for a one-dimensional model.

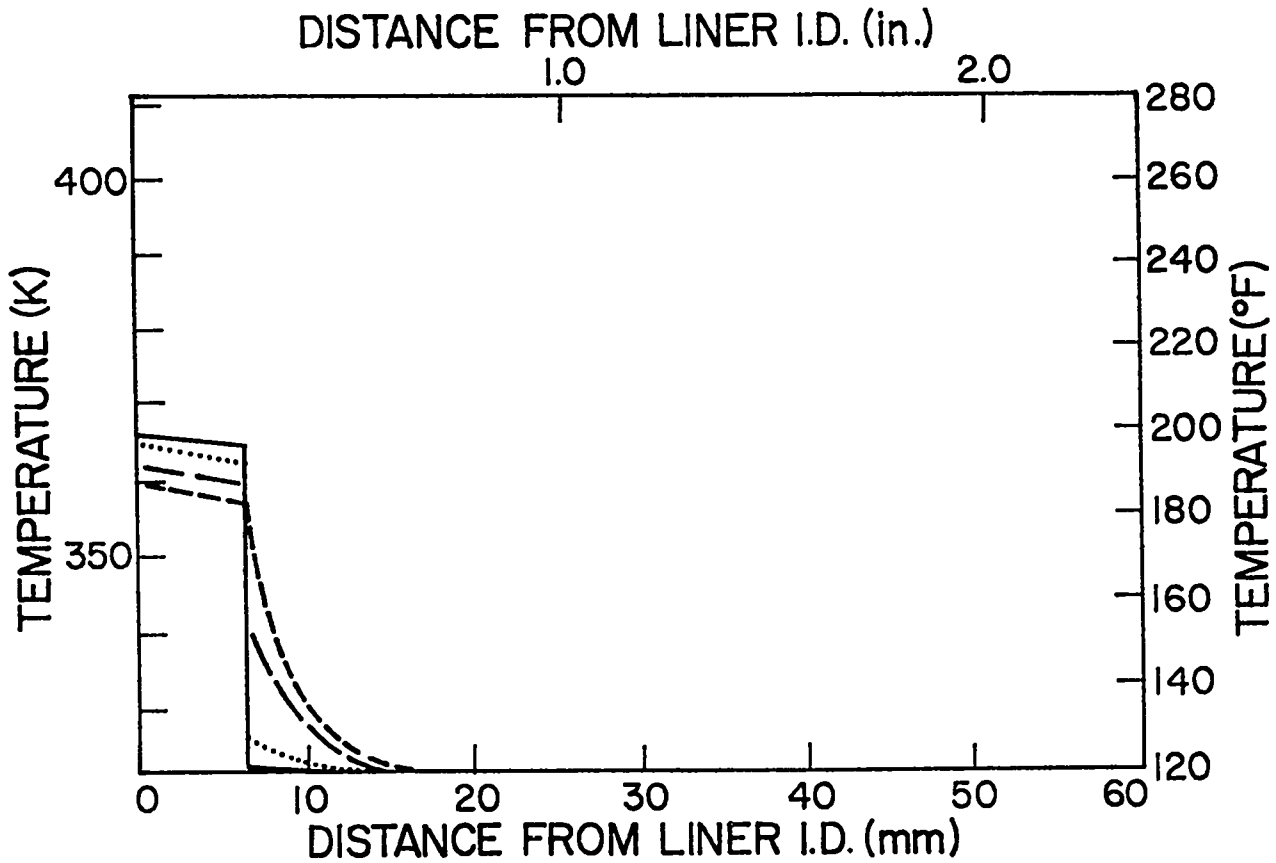


Fig. 7. Effect of H_c on temperature distribution at 30 s for the one-dimensional model.

Curve	Conductance, H_c		(E/A) ,		Absorbed Energy Distribution, %	
	$W/m^2/K$	$Btu/h /ft^2/F$	MJ/m^2	Btu/ft^2	Liner	Concrete
—	5.58	1.	1.01	89	~ 100	~ 0
.....	56.8	10.	1.01	89	97	3
---	568.	100.	1.04	92	87	13
- - -	5680.	1000.	1.08	95	79	21

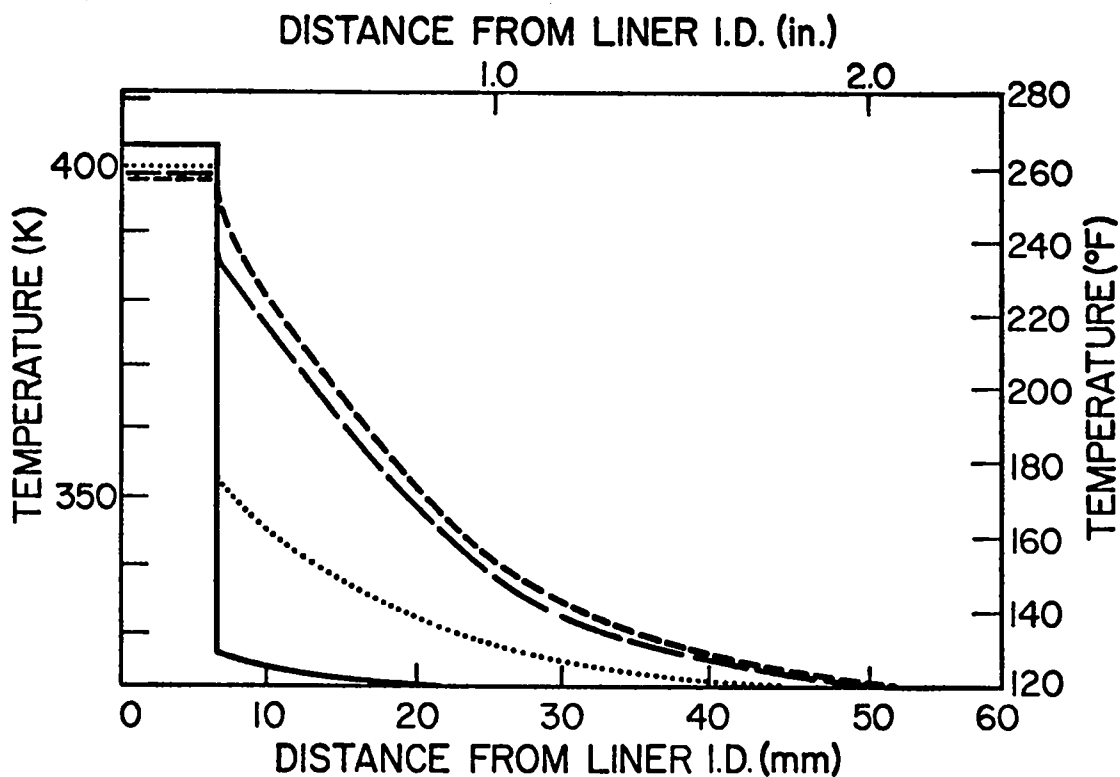


Fig. 8. Effect of H_c on temperature distribution at 300 s for the one-dimensional model.

Curve	Conductance, H_c		(E/A) ,		Absorbed Energy Distribution, %	
	$W/m^2/K$	$Btu/h /ft^2/F$	MJ/m^2	Btu/ft^2	Liner	Concrete
—	5.68	1	2.03	179	94	6
.....	56.8	10	2.64	233	69	31
- - -	568.0	100	3.64	321	47	53
- . - .	5680.0	1000	3.89	343	44	56

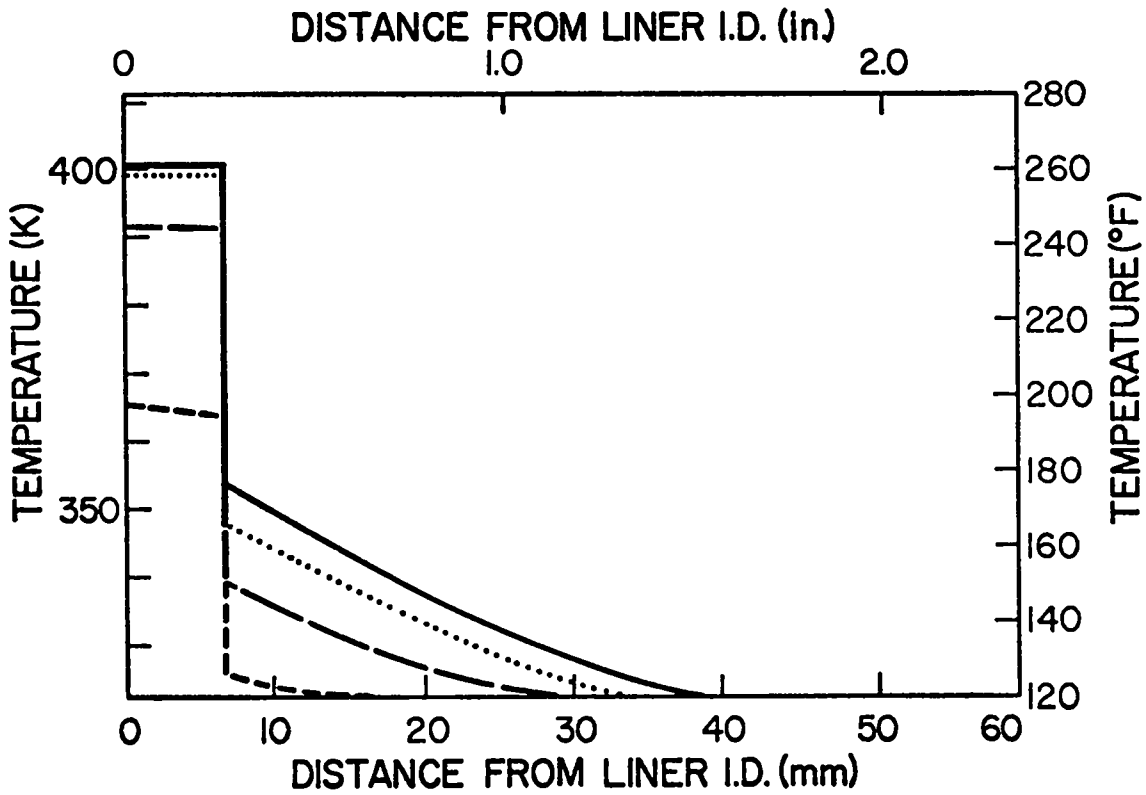
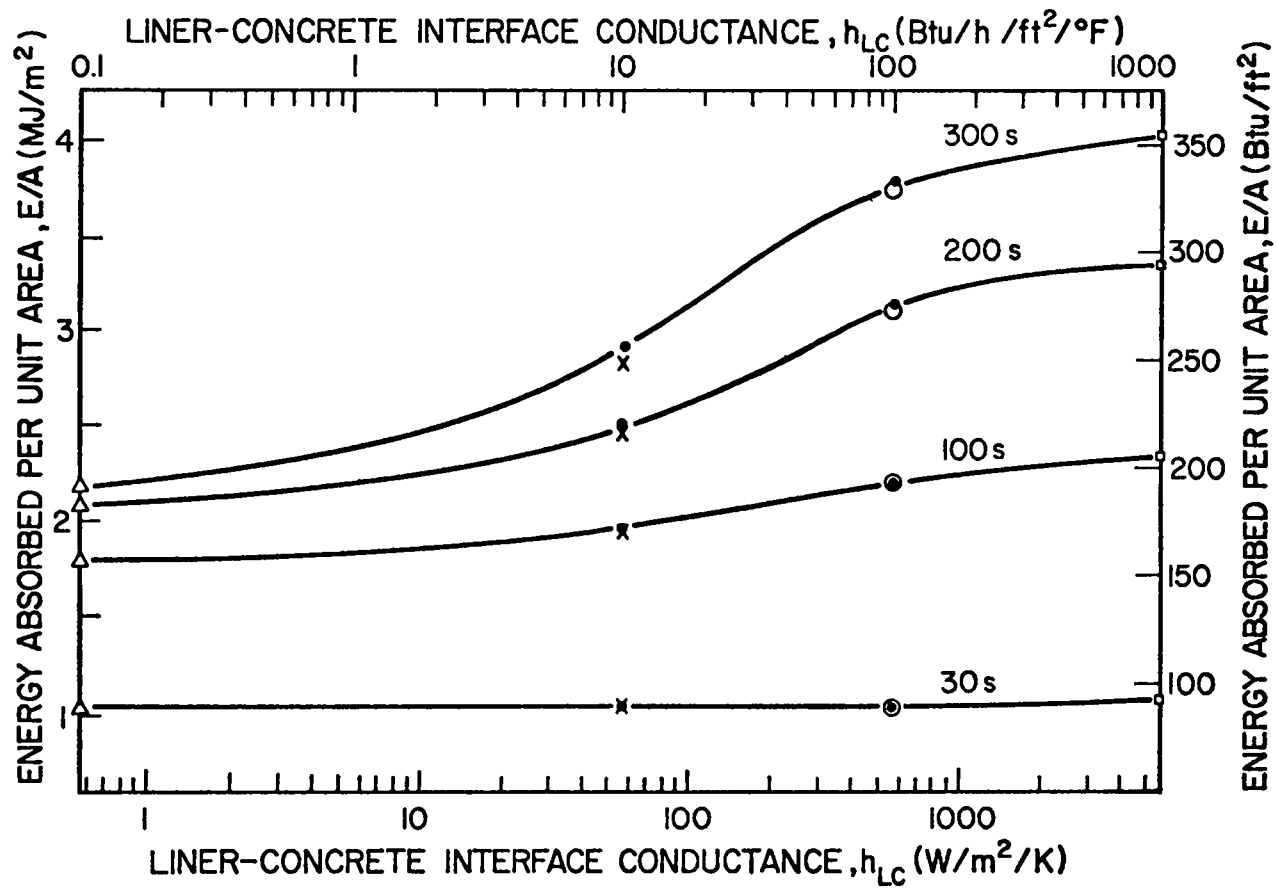


Fig. 9. Effect of time on temperature distribution for $H_c = 57 \text{ W/m}^2/\text{K}$ ($10 \text{ Btu/h/ft}^2/^\circ\text{F}$) for the one-dimensional model.

Curve	Time, s	(E/A),		Absorbed Energy Distribution, %	
		MJ/m ²	Btu/ft ²	Liner	Concrete
—	300	2.64	233	69	31
.....	200	2.34	206	77	23
- - -	100	1.86	164	88	12
- . - .	30	1.01	89	97	3



18 Fig. 10. Effect of h_{LC} and h_{AC} on absorbed energy/area for the two-dimensional model.

Anchor - Concrete
Interface Conductance, h_{AC}

<u>Symbol</u>	<u>W/m²/K</u>	<u>Btu/h /ft²/°F</u>
Δ	0.1	0.568
x	1.0	5.68
o	10.	56.8
·	100.	568.
	1000.	5680.

Fig. 10. (continued)

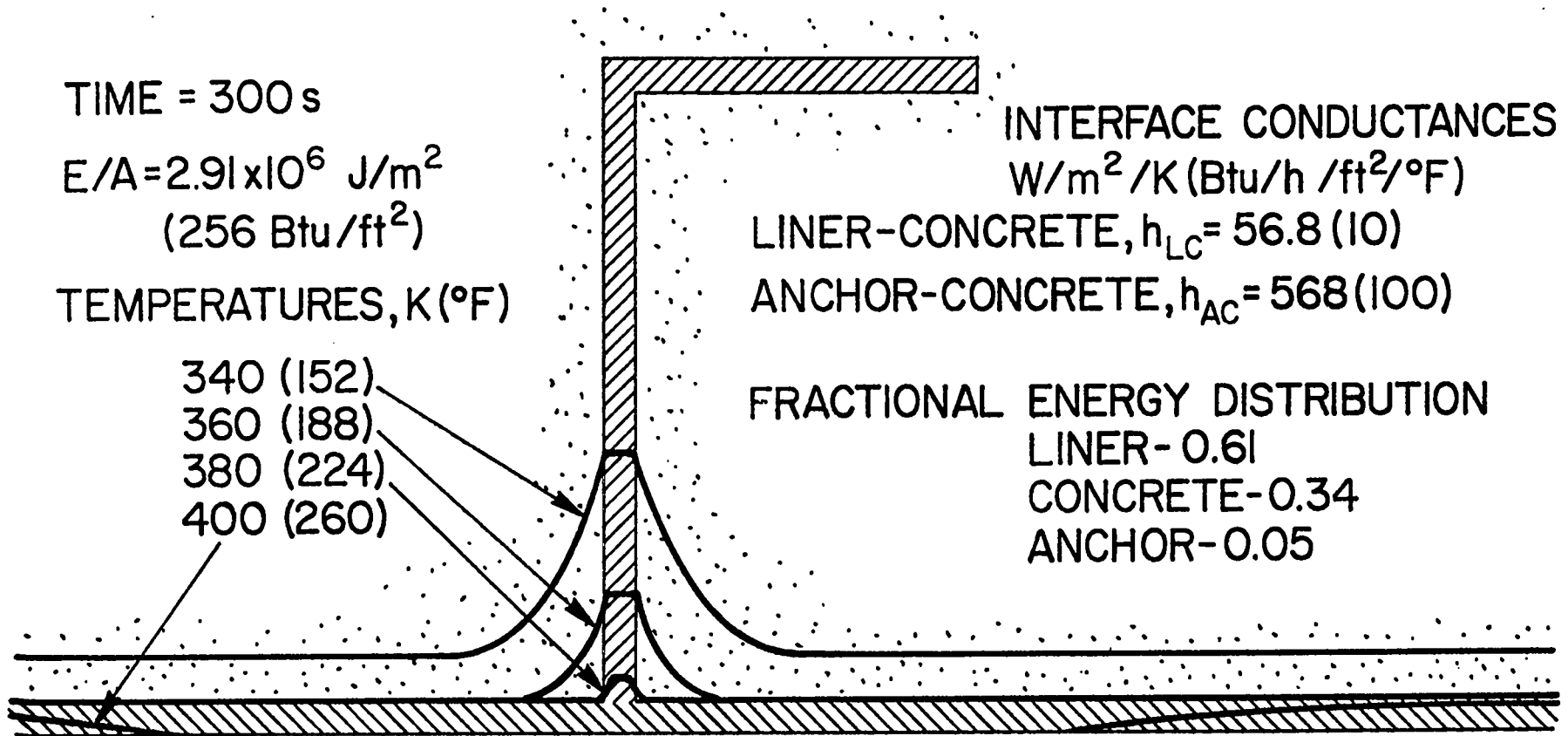


Fig. 11. Two-dimensional model temperature distribution with high anchor-concrete conductance.

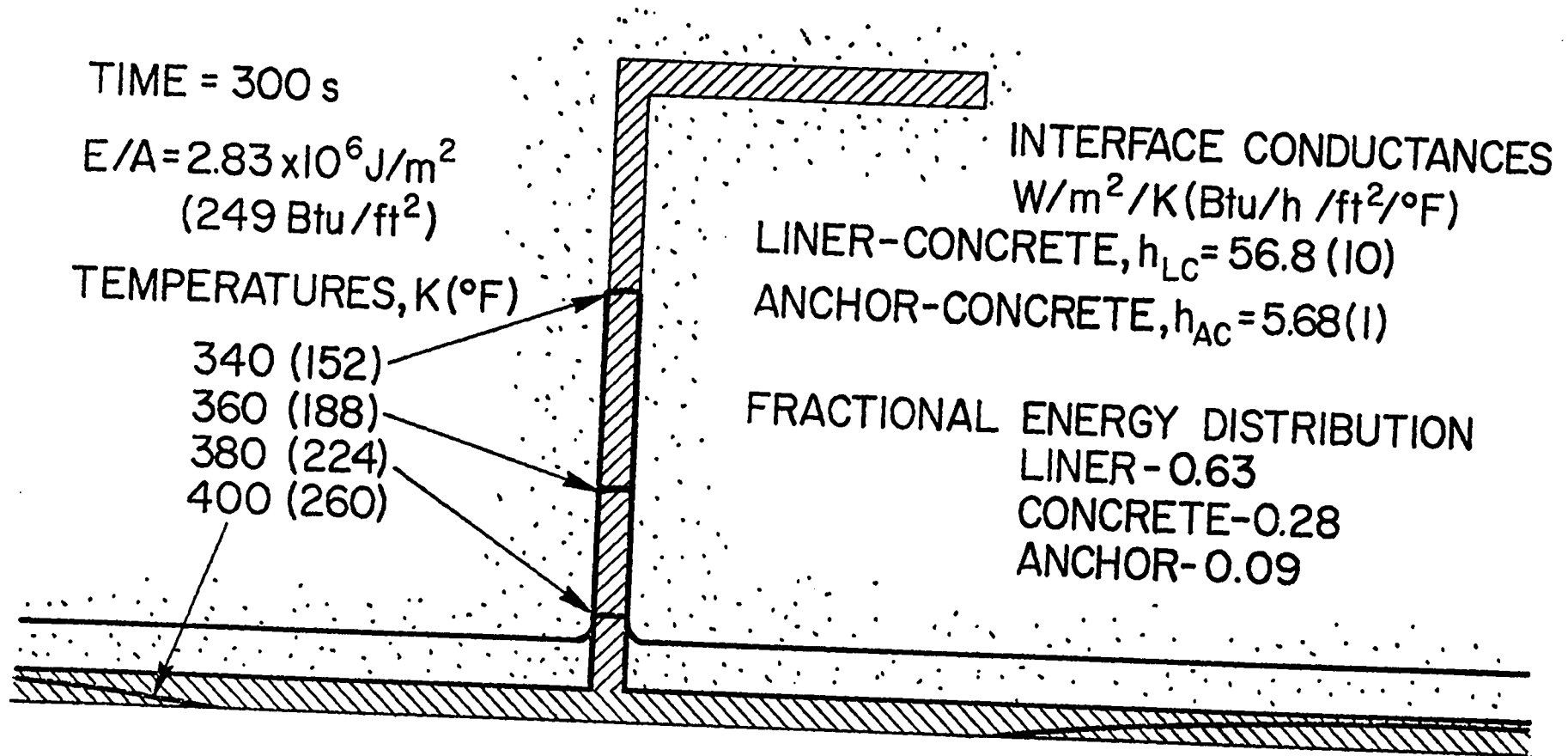


Fig. 12. Two-dimensional model temperature distribution with low anchor-concrete conductance.

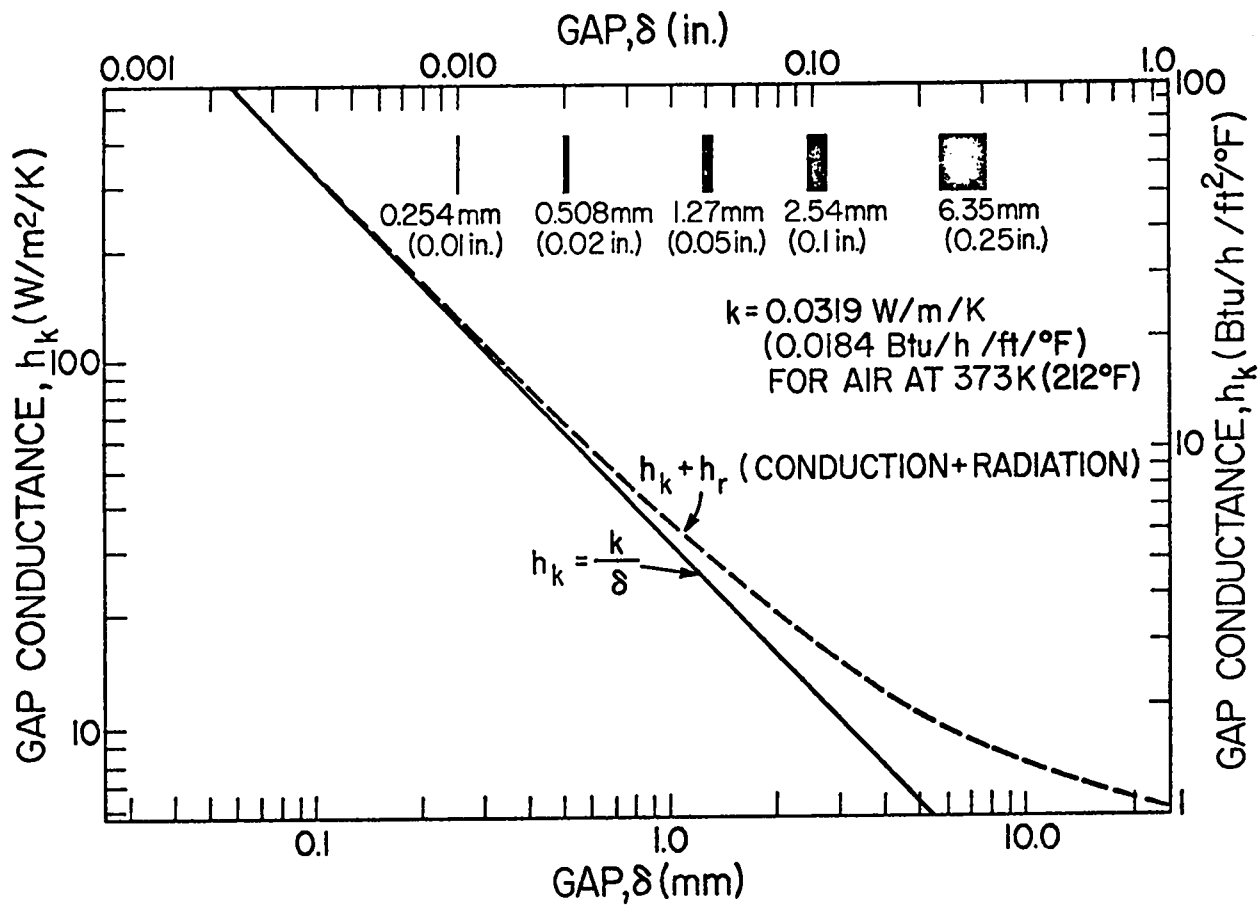


Fig. 13. Gap conductance due to conduction and radiation across an air gap.

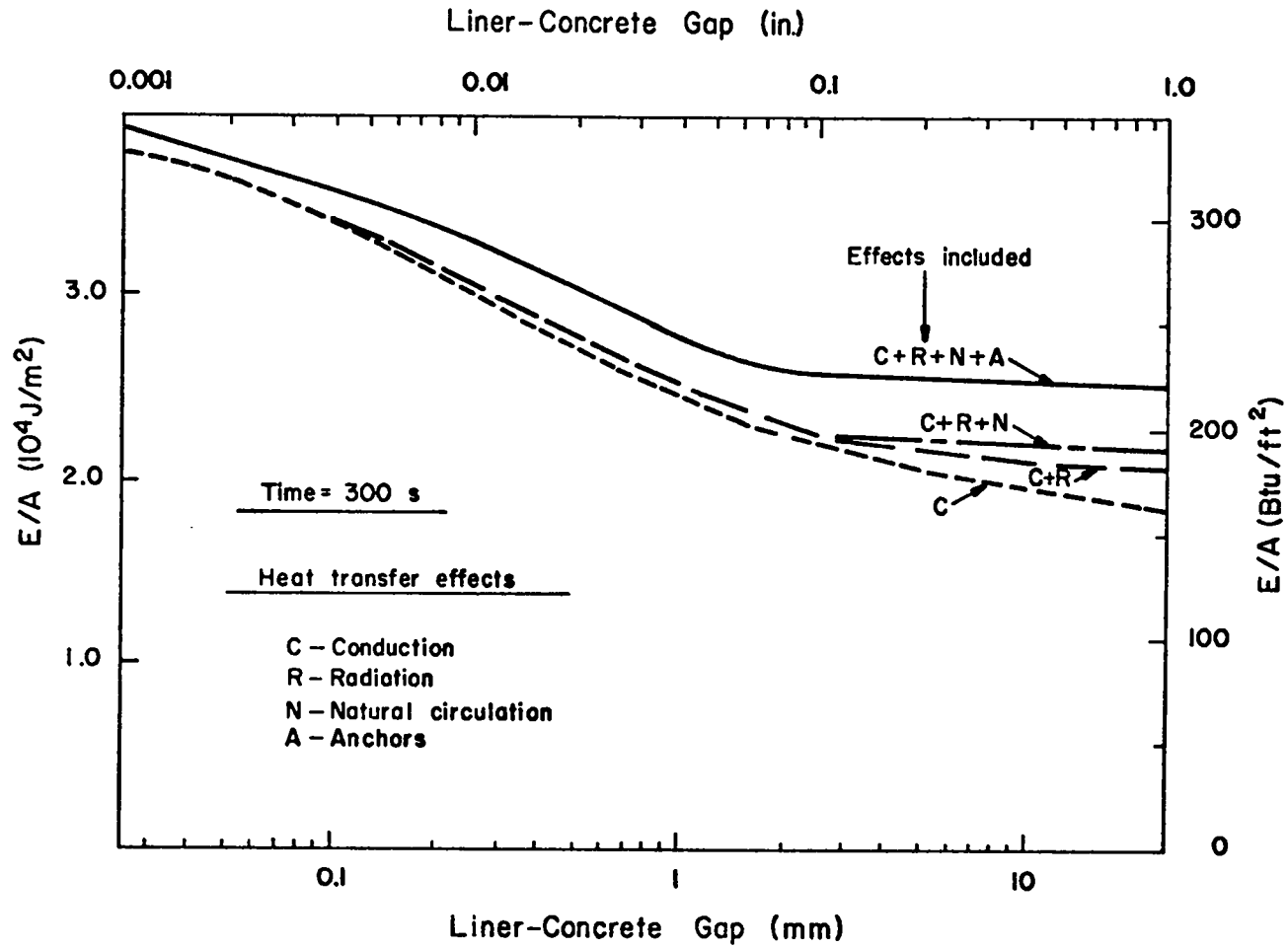
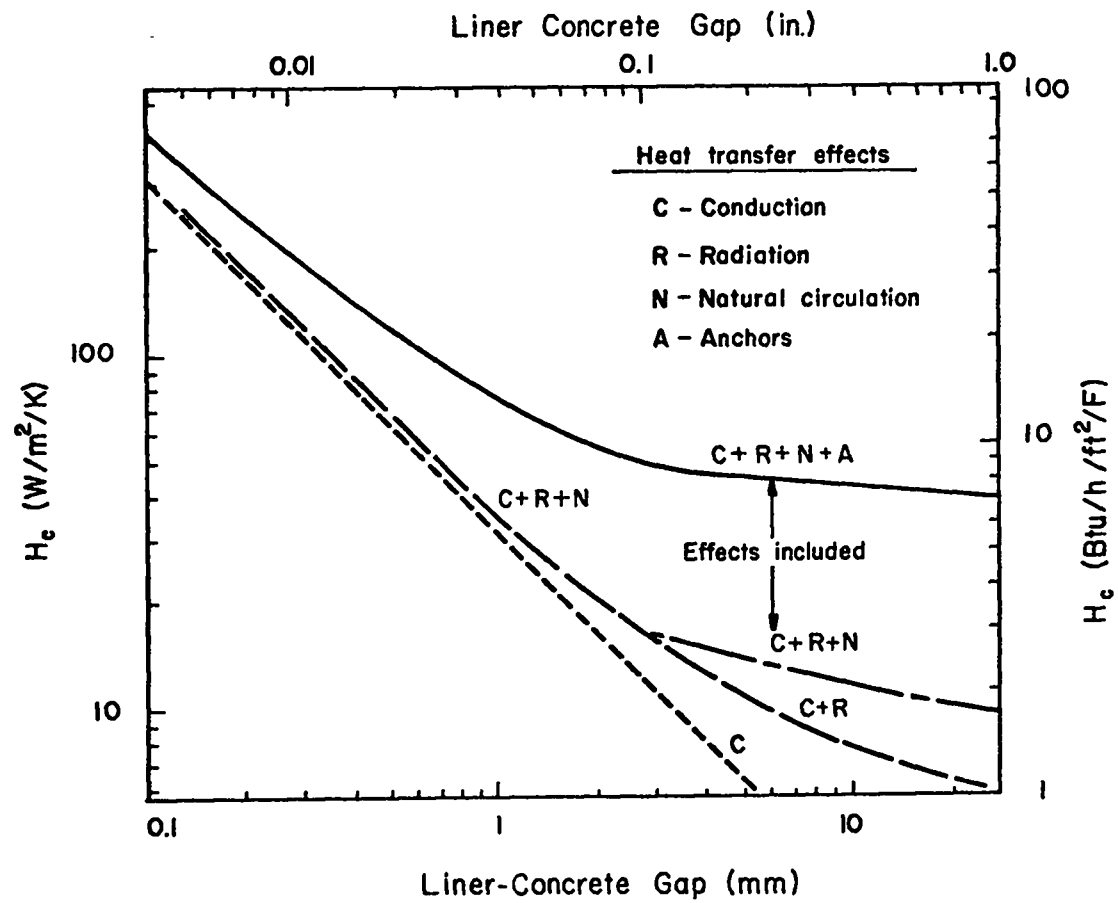
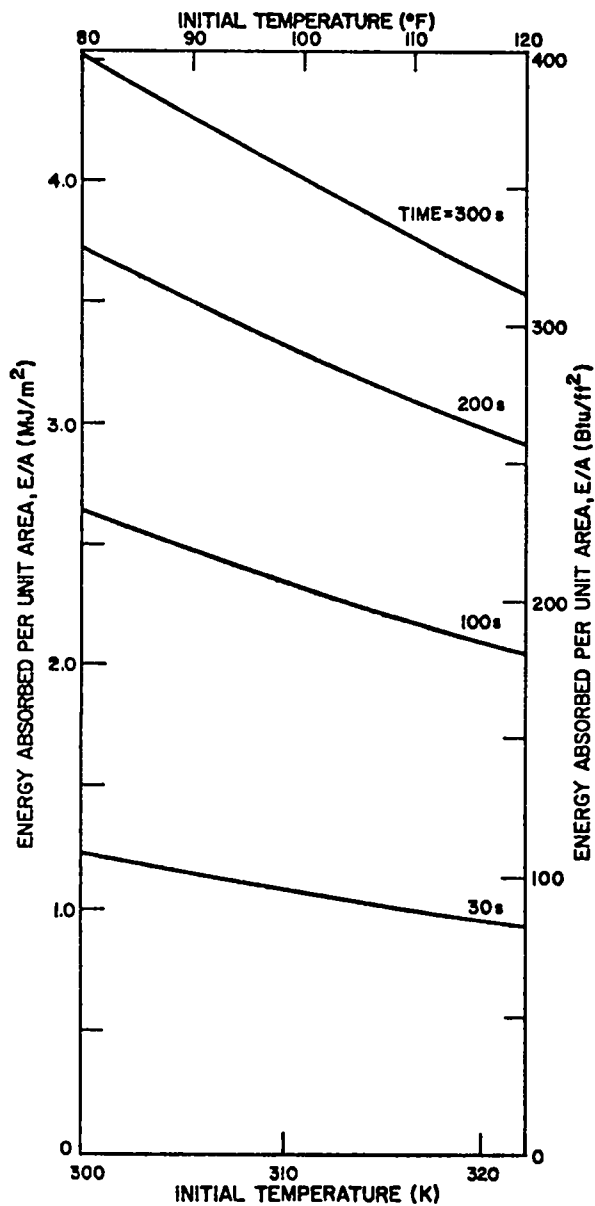


Fig. 14. Heat transfer effects on lined-concrete energy absorbed/area, E/A , after 300 s.



37 Fig. 15. Heat transfer effects on one-dimensional liner-concrete interfacial conductance, H_c .



- Notes: 1. Two-dimensional model
 2. Interface conductances,

Location	Value: $W/m^2/K$ (Btu/h \cdot ft 2 /°F)
Liner-concrete	568 (100)
Anchor-concrete	568 (100)

3. Containment atmosphere boundary conditions, see Fig. 3,

$$h_{ATM} = 568 \text{ W/m}^2/\text{K} (100 \text{ Btu/h} / \text{ft}^2 / \text{°F})$$

$$T_{ATM} = 400 \text{ K} (260\text{°F}).$$

Fig. A-1. Effect of initial temperature on energy absorbed.

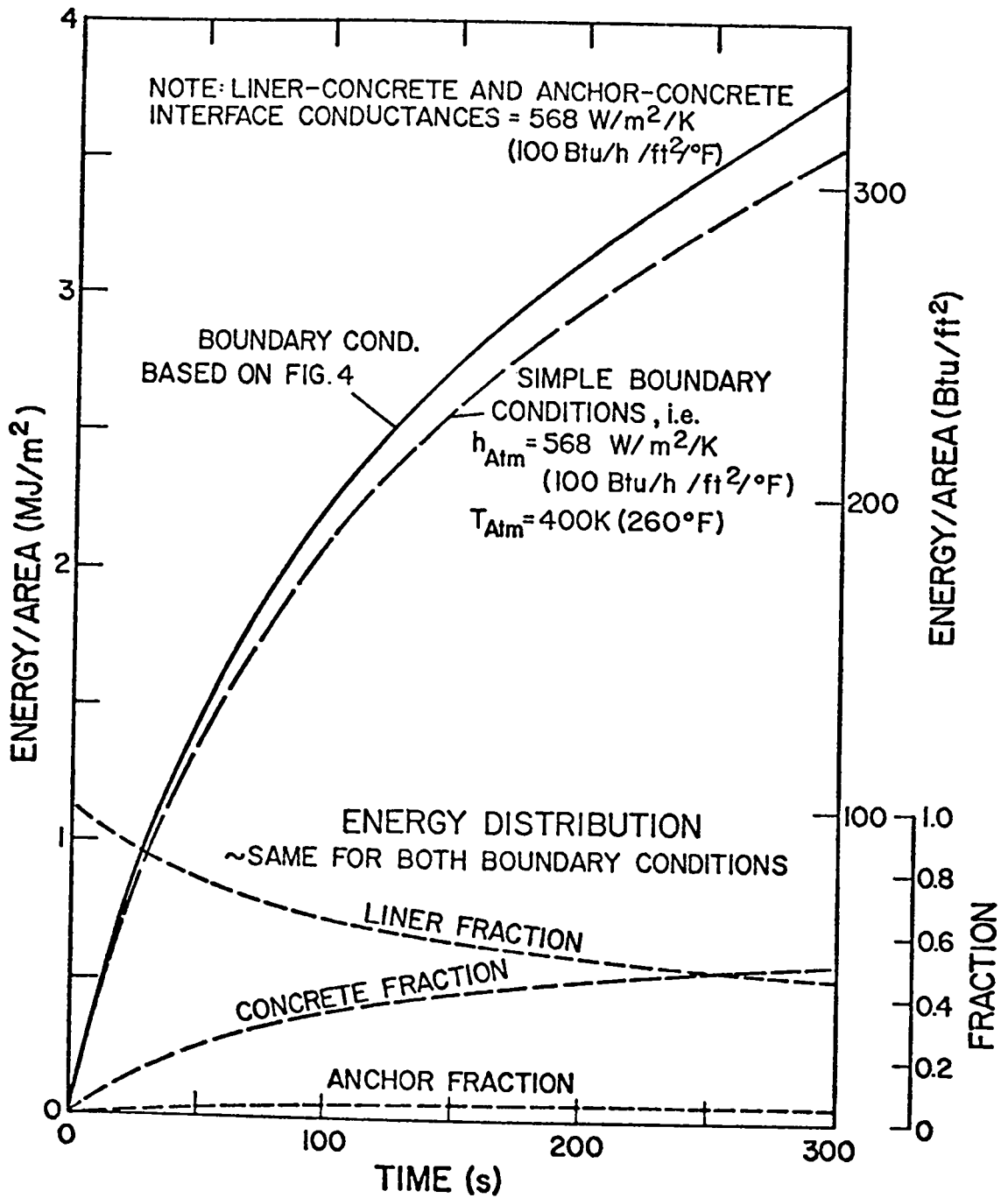


Fig. A-2. Two-dimensional energy absorbed with different boundary conditions.

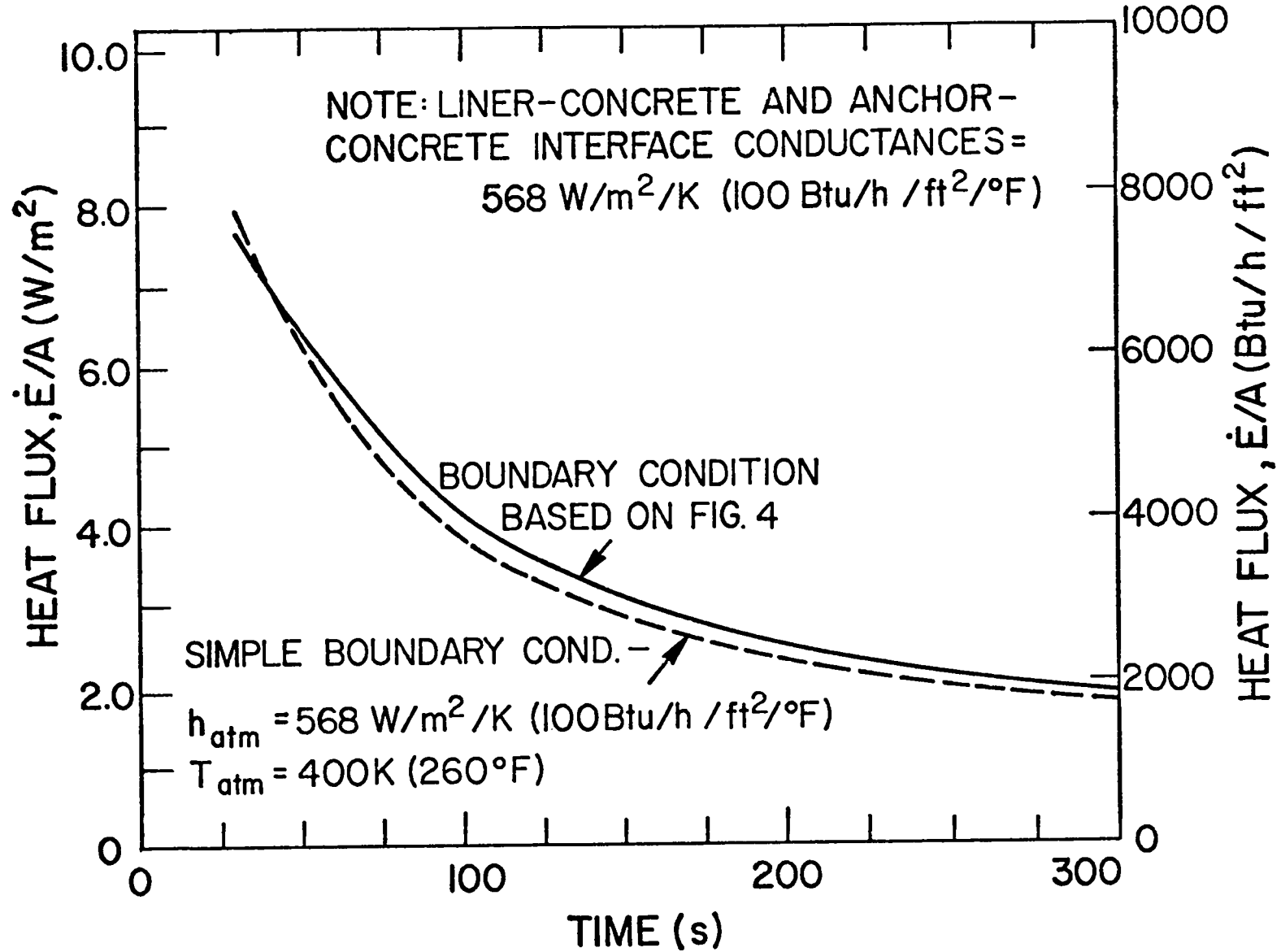


Fig. A-3. Two-dimensional model heat fluxes (\dot{E}/A) with different boundary conditions.

TABLE I
THERMAL PROPERTIES

Material	Density		Conductivity		Heat Capacity		Diffusivity	
	kg/m ³	lbm/ft ³	W/m/K	Btu/h /ft ² /°F	J/kg/K	Btu/lbm/°F	m ² /s	ft ² /h
Liner and Anchor	7.78 x 10 ³	486.	45.	26.	0.11	460.	1.3 x 10 ⁻⁵	0.49
Concrete	2.08 x 10 ³	130.	1.4	0.8	0.23	960.	7.0 x 10 ⁻⁷	0.027

TABLE II

DETERMINATION OF THE EQUIVALENT ONE-DIMENSIONAL LINER-CONCRETE INTERFACE CONDUCTANCE (H_c)
TO GIVE THE SAME ABSORBED ENERGY/AREA (E/A) AS THE
TWO-DIMENSIONAL (WITH ANCHOR) MODEL WITH VARIOUS LINER-CONCRETE INTERFACE CONDUCTANCES (h_{LC}) AT 300 s

2-D h_{LC}			E/A^a		Equivalent 1-D, H_c^b		$\frac{(E/A)_{2D}}{(E/A)_{1D}}$
W/m ² /K	Btu/h ft ² /°F		MJ/m ²	Btu/ft ²	W/m ² /K	Btu/h /ft ² /°F	for same h_{LC}^c
5.7	1		2.38	210	28	5	1.17
57.	10		2.89	255	97	17	1.08
570.	100		3.75	330	1140	200	1.03

^afrom Fig. 10.

^bfrom Fig. 6.

^cfrom Figs. 6 and 10.

TABLE III

EFFECT OF ANCHORS ON THE ENERGY ABSORBED/AREA vs TIME
 FOR $h_{LC} = 56.8 \text{ W/m}^2/\text{K}$ (10 Btu/h ft²/°F)

Time, s	$\frac{(E/A)_{2D}}{(E/A)_{1D}}$
	30
100	1.04
200	1.06
300	1.08

TABLE IV

AIR THERMAL CONDUCTIVITY vs TEMPERATURE

Temperature		Air Thermal Conductivity	
K	°F	W/m/K	Btu/h /ft/°F
273	32	0.0242	0.0140
373	212	0.0319	0.0184
473	392	0.0388	0.0224

TABLE V

EFFECT OF LINER DISPLACEMENT VARIATION ON ENERGY ABSORBED AT 300 s

Displacement, mm (in.)			$\frac{(E/A)_{300 \text{ s}}}{\text{MJ/m}^2 (\text{Btu/ft}^2)}$		
Minimum	Maximum	Mean	Linear Variation	Based on Mean Displacement (Fig. 6)	Difference %
0.0254(0.001)	1.04(0.041)	0.533(0.021)	2.84(250)	2.67(235)	6
0.0254(0.001)	2.06(0.081)	1.04(0.041)	2.64(233)	2.44(215)	8

TABLE A-I

TWO-DIMENSIONAL MODEL:
EFFECT OF MESH SPACING IN DIRECTION NORMAL TO LINER

Fixed Conditions -

- $h_{LC} = h_{AC} = 570 \text{ W/m}^2/\text{K}$ (100 Btu/h /ft²/°F)
- Boundary conditions from Fig. 4
- Initial temperature = 300 K (80°F)

Avg. Energy Absorbed as a % of Total (%T) and Difference Between
Fine and Coarse Mesh Relative to the Avg. (%D).

Time, s	Liner		Concrete		Anchor		Total
	%T	%D	%T	%D	%T	%D	%D
28	86	0.7	12	- 6.8	2	- 2.4	- 2.5
100	64	0.8	33	- 4.4	3	- 2.4	- 0.9
190	53	0.2	44	- 3.0	3	- 1.3	- 1.2

Notes: $\%T_i = 100 \cdot E_i / \bar{E}_i$, $i = \text{liner, concrete, etc.}$

$$\%D_i = 100 \cdot (E_F - E_C)_i / \bar{E}_i$$

E_F = Energy absorbed by fine mesh

E_C = Energy absorbed by coarse mesh

$$\bar{E} = 0.5 (E_F + E_C)$$

- Fine mesh: $\Delta y = 1.3, 2.5, 3.8, \dots \text{ mm}$ (0.05, 0.10, 0.15, ... in.).
See Fig. 3.
- Coarse mesh: $\Delta y = 10, 10, 10, \dots \text{ mm}$ (0.4, 0.4, 0.4, ... in.).

TABLE A-II

ONE-DIMENSIONAL MODEL:
EFFECT OF MESH SPACING IN DIRECTION NORMAL TO LINER

Δy_1^* , mm (in.)	Energy Absorbed/Area at 300 s, E/A,	% Increase in (E/A) Relative to Base Case
	MJ/m^2 (Btu/ft ²)	
1.3 (0.05)	2.645 (233.1)	Base Case
1.8 (0.07)	2.658 (233.3)	0.1
2.8 (0.11)	2.650 (233.5)	0.2
5.8 (0.23)	2.658 (234.2)	0.5
15.0 (0.58)	2.684 (236.5)	1.4

* The mesh spacing is graduated as follows: $\Delta y_1 = \Delta y_1$, $\Delta y_2 = 2\Delta y_1$, $\Delta y_3 = 3\Delta y_1$, etc.

Fixed Conditions:

- $H_c = 57 \text{ W/m}^2/\text{K}$ (10 Btu/h /ft²/°F)
- Boundary conditions from Fig. 4.

TABLE A-III

EFFECT OF TRANSIENT TIME INCREMENT ON ENERGY ABSORBED

Notes:

1. Two-dimensional model
2. Initial temperature = 300 K (80°F)
3. Boundary conditions from Fig. 4.
4. $E_{1/2}$ results use,
 $\Delta t = 1$ s to 30 s
 $\Delta t = 5$ s after 30 s
5. E_1 results use,
 $\Delta t = 2$ s to 30 s
 $\Delta t = 10$ s after 30 s

<u>Time, s</u>	<u>Change in Energy Absorbed,^a %</u>			
	<u>Liner</u>	<u>Concrete</u>	<u>Anchor</u>	<u>Total</u>
28	+ 1.2	- 1.3	+ 0.2	+ 0.8
100	+ 0.8	+ 1.0	+ 0.8	+ 0.9
330	+ 0.1	+ 0.03	+ 0.3	+ 0.2

$$^a 100 (E_1 - E_{1/2}) / \bar{E}$$

$$\bar{E} = 0.5(E_1 + E_{1/2}).$$

TABLE C-1

VERTICAL ENCLOSURE
NATURAL CONVECTION HEAT TRANSFER COEFFICIENTS

At 300 s, One-Dimensional Model, gap height of 1 m (3.3 ft)

Gap, (mm)	t (in.)	Grashof Number	h_{nc} , W/m ² /K (Btu/h /ft ² /°F)	$h_k = k^*/t$, W/m ² /K (Btu/h /ft ² /°F)	Temperatures, K(°F)	
					Liner	Concrete
0.51	0.020	1	**	62 (11)	399 (258)	357 (183)
2.5	0.10	239	**	12 (2.2)	398 (256)	369 (204)
7.6	0.30	7765	4.0 (0.7)	4 (0.7)	404 (267)	326 (127)
25.0	1.0	2.9×10^5	3.4 (0.6)	1 (0.2)	404 (267)	326 (127)

* $k = 0.031$ W/m/K (0.018 Btu/h /ft/°F)

** Conduction predominates, i.e., no natural convection.